Chapter 4

Effect of torrefaction on physicochemical properties of biomass and characterization of torrefaction by-products

4.1 Overview

This chapter is aimed to focus on the quantitative and qualitative aspects of various products from torrefaction of pigeon pea stalk and eucalyptus for which optimum operating conditions of torrefaction have already been discussed in Chapter 3. The present chapter renders the detailed information regarding the effect of torrefaction and its severity on the quantity and the quality of various products (main product: torrefied biomass and by-products: liquid part (condensable gases) and torgas (non-condensable gases (NCG)) obtained from the torrefaction of pigeon pea stalk and eucalyptus. This chapter also addresses few of the drawbacks associated with the solid fuel properties of raw biomass while co-combustion with coal and how torrefaction helps in improving these properties such as flowability, compactibility and combustion indices. The later part of the chapter includes the estimation of kinetic parameters for the pyrolysis of raw and torrefied biomass using thermogravimetric analysis data in the direct Arrhenius equation plot method with an assumption of three pseudo-components.

4.2 Characterization methods

Moisture content (M) in proximate analysis has been calculated using the ASTM standards D-871-82 and ash content (ASH) for biomass has been calculated following the ASTM test protocol E-1755-01. During the determination of volatile matter (VM)

for biomass ASTM D-346 standards has been followed. The fixed carbon (FC) present in the biomass has been determined using Eq. (4.1):

$$\mathbf{FC = 100 - (M + VM + ASH)} \quad (4.1)$$

The elemental analyzer Eurovector (EuroEA3000) has been used in order to determine the elemental composition (C, H, N, S and O by difference) of various products. However, the sulfur content could not be obtained as it has been below the detection limit of the instrument.

To calculate the HHV, a bomb calorimeter (Rajdhani Scientific Instruments Co., New Delhi, R-S-B-3/2204-7-3) has been used with standard UNE-EN 14918:2011 being followed during the procedure.

The composition (hemicellulose, cellulose, and lignin) of raw and torrefied biomass have been determined by using the protocol, as mentioned by Bledzki et al. (Bledzki et al., 2010). The extractive part has been calculated by difference.

SEM (Evo 18 Research, Carl Zeiss, and Oxford Instruments) has been used to examine the physical changes in torrefied biomass as compared to their respective raw biomass. The functional groups present in raw and torrefied biomass have been detected by using FTIR (Thermo Electron Corporation, USA) and the frequency range has been kept 4000 to 400 cm^{-1}. Water content in the liquid product of torrefaction has been measured using Karl Fischer titrimetric method (company- Microprocessor KF moisture titrator and model no- 1760).

The pyrolysis behavior of raw and torrefied biomass have been examined by using TGA which has been carried out on the Pyris 1, Perkin Elmer with test samples varying from 7-10 mg at a constant heating rate (15 °C/min) under nitrogen atmosphere (flow

rate maintained at 50 mL/min) and the temperature range varying from ambient temperature to 800 °C.

The non-condensable gases have been sampled in Tedlar bags and analyzed offline using a gas chromatograph (Centurion Scientific CS5800, New Delhi) on TCD equipped with a stainless steel column (Carbosieve S-II). Argon has been used as a carrier gas and gas chromatograph programmed at 60, 80 and 150 °C for oven, injector and TCD temperature, respectively. The volume concentrations of gas product has been calculated on nitrogen free basis and total volume of nitrogen (after heating starts) used during torrefaction has been measured with the help of mass flow controller (MFC), Bronkhorst-EL-FLOW SELECT F-210CV.

The chemical composition of liquid product has been analyzed using GC/MS (Shimadzu QP-2010 plus). Column used for GC/MS analysis is -RXi-5 Sil MS (30 m X 0.25 mm X 0.25 µm). The oven has been programmed at an initial of 50 °C, then heated up to 250 ^{o}C at 5 ^{o}C/min with holding time of 5 minutes and then again heated up to 280 ^{o}C at 10 ^{o}C/min with holding time of 5 minutes. Injection temperature has been programmed at 260 ^{o}C with split ratio of 10:1. Helium has been used as acarrier gas at a flow rate of 1.21 mL/min. The peaks obtained have been identified by using the National Institute of Standards and Technology library (NIST, USA).

In order to measure the tapped and the loose bulk density, the procedure, as mentioned in Tannous et al. (Tannous et al., 2013) has been followed. The procedure includes the introduction of biomass (2-4 g) into a pre-weighed dry measuring cylinder using a funnel, and no compacting being done. The volume of the biomass has been read off directly from the measuring cylinder and the weight of the cylinder containing the

biomass has been measured using a weighing balance with precision up to 0.1 mg. The loose bulk density has been given by Eq. (4.2):

$$\rho_{Lb} = \frac{m_{cs} - m_c}{V_{Lb}} \quad (4.2)$$

The same procedure for tapped bulk density has been followed as mentioned for loose bulk density, with the only difference being that after introducing the biomass, the measuring cylinder has been tapped at least 100 times or until the volume reaches a constant value. The tapped bulk density has been given by Eq. 4.3:

$$\rho_{Tb} = \frac{m_{cs} - m_c}{V_{Tb}} \quad (4.3)$$

The flowability of the raw and torrefied biomass have been studied using the Hausner Ratio (HR) as given in Eq. (4.4):

$$HR = \frac{\rho_{Tb}}{\rho_{Lb}} \quad (4.4)$$

Samples having HR values ranging from 1.2 to 1.4 have good flow properties (Conag et al., 2017).

The compactibility of the raw and torrefied biomass have been studied using the Carr Compressibility Index (CCI) as given by Eq. (4.5):

$$CCI\ (\%) = \left(1 - \frac{\rho_{Lb}}{\rho_{Tb}}\right) \times 100 \quad (4.5)$$

The energy density (MJ/m^3) has been calculated by using Eq. (4.6):

$$\text{Energy density} = HHV \times \text{Loose bulk density} \quad (4.6)$$

HHV_{db} has been calculated using Eq. (4.7):

$$HHV_{db} = \frac{HHV \times 100}{100 - M} \quad (4.7)$$

The combustion indices (FR, CI, and VI) of raw and torrefied eucalyptus have been calculated using Eq. (4.8)-(4.10) (Conag et al., 2017; Singh et al., 2019):

$$\mathbf{FR} = \frac{\mathbf{FC_{db}}}{\mathbf{VM_{db}}} \tag{4.8}$$

$$\mathbf{CI} = \mathbf{HHV_{db}} \times (\mathbf{115} - \mathbf{Ash_{db}}) \times \frac{\mathbf{1}}{\mathbf{105} \times \mathbf{FR}} \tag{4.9}$$

$$\mathbf{VI} = \frac{\mathbf{HHV_{db}} - \mathbf{0.338\ FC_{db}}}{\mathbf{VM_{db}} + \mathbf{M_{db}}} \times \mathbf{100} \tag{4.10}$$

In the case of moisture reabsorption test for raw and torrefied biomass approximately 1 g of each sample has been taken in a separate pre-dried petri dish and placed in an oven at 103-105 ^{o}C for 3-4 hrs to remove any inherent moisture. The dried samples have been weighed and their initial dried weight has been determined. The samples have been then exposed to atmospheric conditions and weight has been noted down at a predetermined time intervals (every 24 hrs.) for the duration of 168 hrs. The increase in weight is due to the moisture reabsorption by biomass samples. Relative humidity (RH) and temperature have been monitored and determined using a digital thermo hygrometer (HTC 103-CTH, Mumbai, India) with measurements carried out simultaneously at equal time intervals when the samples have been weighed.

4.3 Calculation method opted for estimating kinetic parameters

Biomass undergoing thermal decomposition during pyrolysis releases volatiles. Lignocellulose biomass mainly consists of hemicellulose, cellulose, and lignin with all showing different thermal behaviors. During biomass thermal decomposition, hemicellulose can be illustrated with a shoulder present in the differential thermogravimetric (DTG) curve with cellulose being represented with the pyrolysis peak (Várhegyi et al., 1997) and lignin showing thermal degradation over a broader range of temperature. In present work, the kinetic analysis has been performed using an independent parallel reaction scheme with three-pseudo components representing hemicellulose, cellulose, and lignin. One of the advantages of using this model over

other models is that it does not essentially require testing the fuel at different heating rates. This is because the heating rate in the range of 3 to 108 ^{o}C/min does not have much effect on the values of activation energy, reaction order, and pre-exponential factors (Bach et al., 2014; Bach et al., 2017; Branca et al., 2005). Also, there are several studies which predicted the kinetic parameters based on a single heating rate (Bach et al., 2014; Bach et al., 2017; Branca et al., 2005; Burra and Gupta, 2019; Gupta et al., 2020; Martín-Lara et al., 2016; Martín-Lara et al., 2017; Yuan et al., 2019). The pseudo-component model uses three parallel and independent reaction given as in Eq. (4.11)-(4.13):

Hemicellulose —> Volatiles $_1$ + Char $_1$ (4.11)

Cellulose —> Volatiles $_2$ + Char $_2$ (4.12)

Lignin —> Volatiles $_3$ + Char $_3$ (4.13)

There are three methods integral, differential, and special methods which are mostly used for estimating kinetic parameters. Differential methods use both mass loss and rate of mass loss, whereas integral methods use only mass loss. In the present study, estimation of kinetic parameters (pre-exponential factor, the order of reaction, and activation energy) has been calculated using TG/DTG data. The present study uses the direct Arrhenius Equation plot method with an assumption of the three-pseudo component undergoing nth order reactions. The thermal decomposition of raw and torrefied biomass can be expressed by Eq. (4.14):

$$\frac{d\alpha_i}{dt} = k(1-\alpha_i)^n, \; i = 1, 2, 3. \quad (4.14)$$

Where α is calculated using Eq. (4.15):

$$\alpha = \frac{m_o - m_t}{m_o - m_f} \quad (4.15)$$

In Eq. (4.14) 'k' has been the temperature dependent rate constant and can be described by Arrhenius equation given in Eq. (4.16):

$$\mathbf{k = Ae^{\frac{-E}{RT}}} \quad (4.16)$$

Taking logarithm on both sides of Eq. (4.16), we get Eq. (4.17):

$$\mathbf{\ln k = \ln A_i - \frac{E_i}{RT}} \quad \mathbf{, i=1, 2, 3} \quad (4.17)$$

The plot between ln k vs. 1/T gives the value of A and E. The Eq. (4.18) gives the overall conversion rate and the Eq. (4.19) gives the overall activation energy (E_T) in the following equation:

$$\mathbf{\frac{d\alpha}{dt} = \sum_{i=1}^{3} C_i \frac{d\alpha_i}{dt} = C_1 \frac{d\alpha_1}{dt} + C_2 \frac{d\alpha_2}{dt} + C_3 \frac{d\alpha_3}{dt}} \quad (4.18)$$

$$\mathbf{E_T = \sum_{i=1}^{3} C_i E_i = C_1 E_1 + C_2 E_2 + C_3 E_3} \quad (4.19)$$

Where C_i represents the contribution factor and is defined as the volatile fraction produced by each component (hemicellulose, cellulose, and lignin) during the thermal decomposition of raw and torrefied biomass.

4.4 Effect of operating parameters on the product distribution during the torrefaction of biomass

The products of torrefaction are solid, liquid and gas where the primary product is solid (torrefied biomass), while byproducts are condensable (liquid) and torgas (NCG). The yield of each product depends heavily on operating parameters such as temperature, heating rate and residence time. Figs. 4.1 (a) and (b) represents the variation of solid, liquid and NCG yield during the torrefaction of pigeon pea stalk and eucalyptus, respectively, with varying final temperature, residence time and heating rate.

(a)

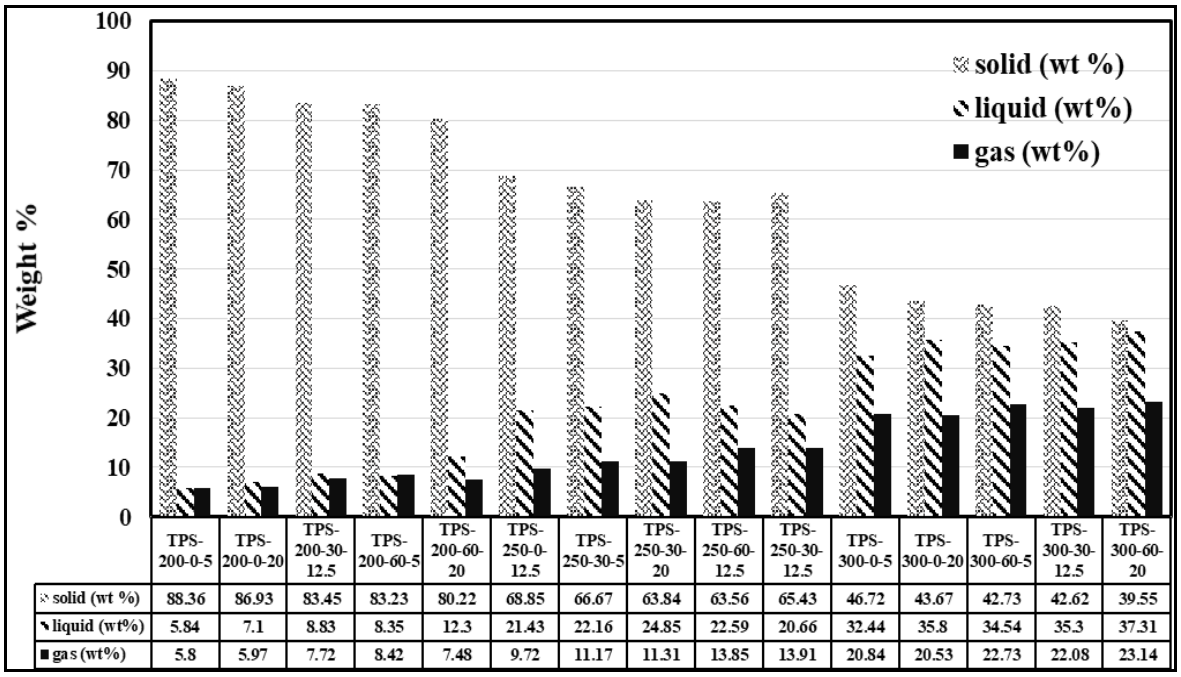

	TPS-200-0-5	TPS-200-0-20	TPS-200-30-12.5	TPS-200-60-5	TPS-200-60-20	TPS-250-0-12.5	TPS-250-30-5	TPS-250-30-20	TPS-250-60-12.5	TPS-250-30-12.5	TPS-300-0-5	TPS-300-0-20	TPS-300-60-5	TPS-300-30-12.5	TPS-300-60-20
solid (wt %)	88.36	86.93	83.45	83.23	80.22	68.85	66.67	63.84	63.56	65.43	46.72	43.67	42.73	42.62	39.55
liquid (wt%)	5.84	7.1	8.83	8.35	12.3	21.43	22.16	24.85	22.59	20.66	32.44	35.8	34.54	35.3	37.31
gas (wt%)	5.8	5.97	7.72	8.42	7.48	9.72	11.17	11.31	13.85	13.91	20.84	20.53	22.73	22.08	23.14

(b)

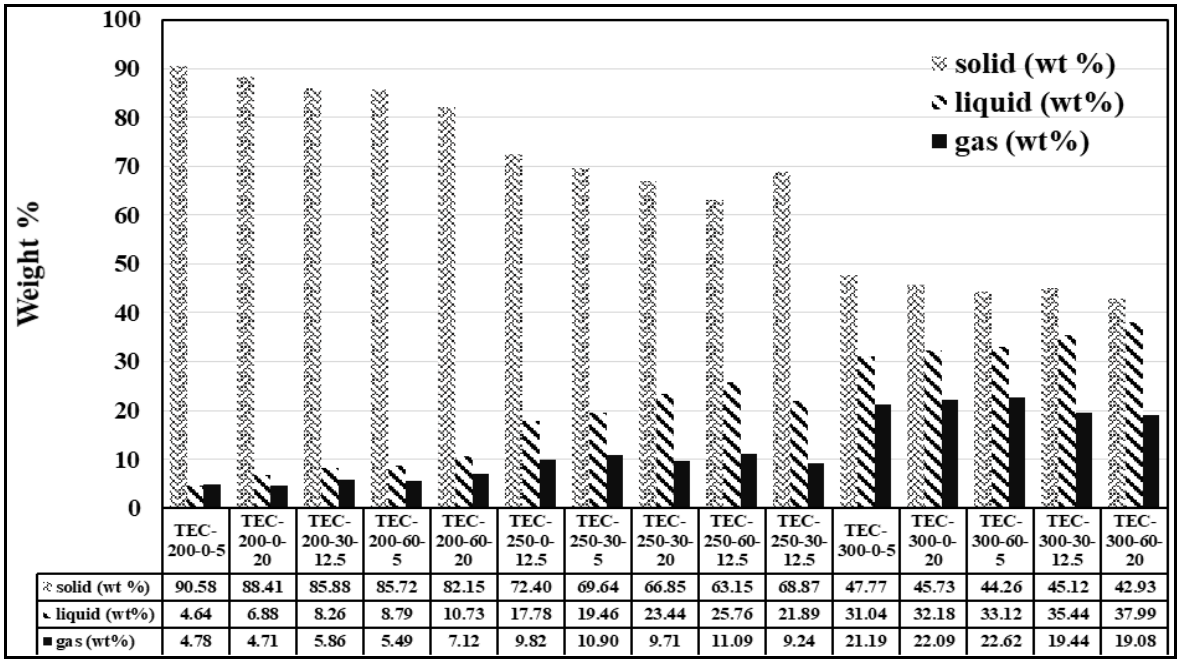

	TEC-200-0-5	TEC-200-0-20	TEC-200-30-12.5	TEC-200-60-5	TEC-200-60-20	TEC-250-0-12.5	TEC-250-30-5	TEC-250-30-20	TEC-250-60-12.5	TEC-250-30-12.5	TEC-300-0-5	TEC-300-0-20	TEC-300-60-5	TEC-300-30-12.5	TEC-300-60-20
solid (wt %)	90.58	88.41	85.88	85.72	82.15	72.40	69.64	66.85	63.15	68.87	47.77	45.73	44.26	45.12	42.93
liquid (wt%)	4.64	6.88	8.26	8.79	10.73	17.78	19.46	23.44	25.76	21.89	31.04	32.18	33.12	35.44	37.99
gas (wt%)	4.78	4.71	5.86	5.49	7.12	9.82	10.90	9.71	11.09	9.24	21.19	22.09	22.62	19.44	19.08

Fig. 4.1 Product distribution during the torrefaction of (a) pigeon pea stalk and (b) eucalyptus, at different operating parameters

On analyzing Fig. 4 it can be observed that as the severity increases during torrefaction the solid yield decreases significantly for both pigeon pea stalk and eucalyptus such as

the solid yield has been decreased continuously from 88.36 (TPS-200-0-5) and 90.58 wt.% (TEC-200-05) to 63.84 (TPS-250-30-20), 39.55 (TPS-300-60-20), and 66.85 (TEC-250-30-20), 42.93 wt.% (TEC-300-60-20). This decrease in solid yield has been mainly due to release of surface and bound moisture (decomposition of hydroxyl groups as confirmed in FTIR analysis) in the initial phase followed by partial to major decomposition of hemicellulose during mild to moderate torrefaction (as confirmed in TGA and DTG). Whereas, for severe torrefaction, partial decomposition of cellulose also happens which results into lesser solid yield (Chen et al., 2018a; Ma et al., 2015). In Fig. 4.1 for both the biomass the gaseous fraction increases for the most severe condition mainly due to the secondary decomposition of condensable vapors formed during high temperature torrefaction.

One can also observe that among three operating parameters of torrefaction, temperature has the most prominent effect as compared to residence time and heating rate on product distribution for both the biomass. This can be confirmed by comparing data such as for TPS-200-30-12.5 (83.45, 8.83 and 7.72 wt.%) to TPS-250-30-12.5 (65.43, 20.66 and 13.81 wt.%) and TPS-300-30-12.5 (42.62, 35.3 and 22.08 wt.%) where temperature at constant residence time and heating rate has significant impact on product distribution. Phanphanich et al. (Phanphanich and Mani, 2011) and Medic et al. (Medic et al., 2012) also mentioned similar trend that torrefaction temperature had the more significant effect on yield and quality of final product obtained. Mundike et al. (Mundike et al., 2016) also mentioned that during torrefaction higher the temperature more was the instability of oxygenated group which resulted in release of more volatiles, consequently giving less solid yield with increased HHV. Based on these discussions it can inferred that for any biomass torrefaction at high temperature is not

suitable as this increases yield of liquid and torgas (NCG) which have less economic value as compared to solid product.

4.5Effect of torrefaction on HHV and proximate analysis of biomass

Table 4.1 Variation of proximate analysis, HHV and bulk density of torrefied biomass with the severity of torrefaction

Sample	Moisture Content (wt.%)	Ash content (wt.%)	Volatile Content (wt.%)	Fixed carbon (wt.%)	HHV (MJ/kg)	Loose bulk density (kg/m^3)	Tapped bulk density (kg/m^3)
RPS	5.43 (0)	1.49 (1.58)	82.12 (86.84)	10.96 (11.59)	16.67	162.3	239.4
TPS-200-0-5	3.21 (0)	1.62 (1.67)	78.43 (81.03)	16.74 (17.30)	17.84	160.11	235.8
TPS-200-30-12.5	2.88 (0)	1.77 (1.82)	75.43 (77.67)	19.92 (20.51)	18.48	155.3	231.9
TPS-250-30-12.5	1.78 (0)	2.68 (2.73)	67.27 (68.49)	28.27 (28.78)	20.58	142.6	195.8
TPSO	1.67 (0)	2.93 (2.98)	65.83 (66.95)	29.57 (30.07)	20.89	141.4	194.3
TPS-300-30-12.5	1.44 (0)	3.57 (3.62)	46.96 (47.65)	48.03 (48.73)	23.73	126.7	167.5
TPS-300-60-20	1.38 (0)	3.76 (3.81)	44.78 (45.41)	50.08 (50.78)	24.23	123.8	163.6
REC	4.23 (0)	0.58 (0.61)	81.20 (84.79)	13.99 (14.61)	17.80	251.70	361.80
TEC-200-0-5	2.58 (0)	0.63 (0.65)	79.73 (81.84)	17.06 (17.51)	18.66	245.78	352.89
TEC-200-30-12.5	2.31 (0)	0.76 (0.78)	76.36 (78.17)	20.57 (21.06)	18.93	240.88	342.37
TEC-250-30-12.5	1.40 (0)	1.13 (1.15)	64.32 (65.23)	33.15 (33.62)	20.98	223.51	313.84
TECO	1.36 (0)	1.16 (1.18)	64.27 (65.16)	33.21 (33.67)	21.34	222.67	311.06
TEC-300-30-12.5	0.92 (0)	1.81 (1.83)	49.66 (50.12)	47.61 (48.05)	24.24	208.05	289.17
TEC-300-60-20	0.90 (0)	2.24 (2.26)	46.98 (47.41)	49.88 (50.33)	24.83	206.01	285.44
Indian Bituminous coal (Bharath et al., 2018)	5.4 (0)	36.4 (38.5)	28.7 30.3)	29.5 (31.2)	-	-	-

Table 4.1 represents the proximate analysis, HHV and bulk density for torrefied pigeon pea stalk and eucalyptus at their respective optimum condition (TPSO and TECO) in comparison with their corresponding raw biomass along with at different torrefaction severity conditions. Fig. 4.1 on the other side gives the graphical representation for the impact of torrefaction in proximate analysis and the same has been compared with the proximate values of Indian grade bituminous coal (Bharath et al., 2018).

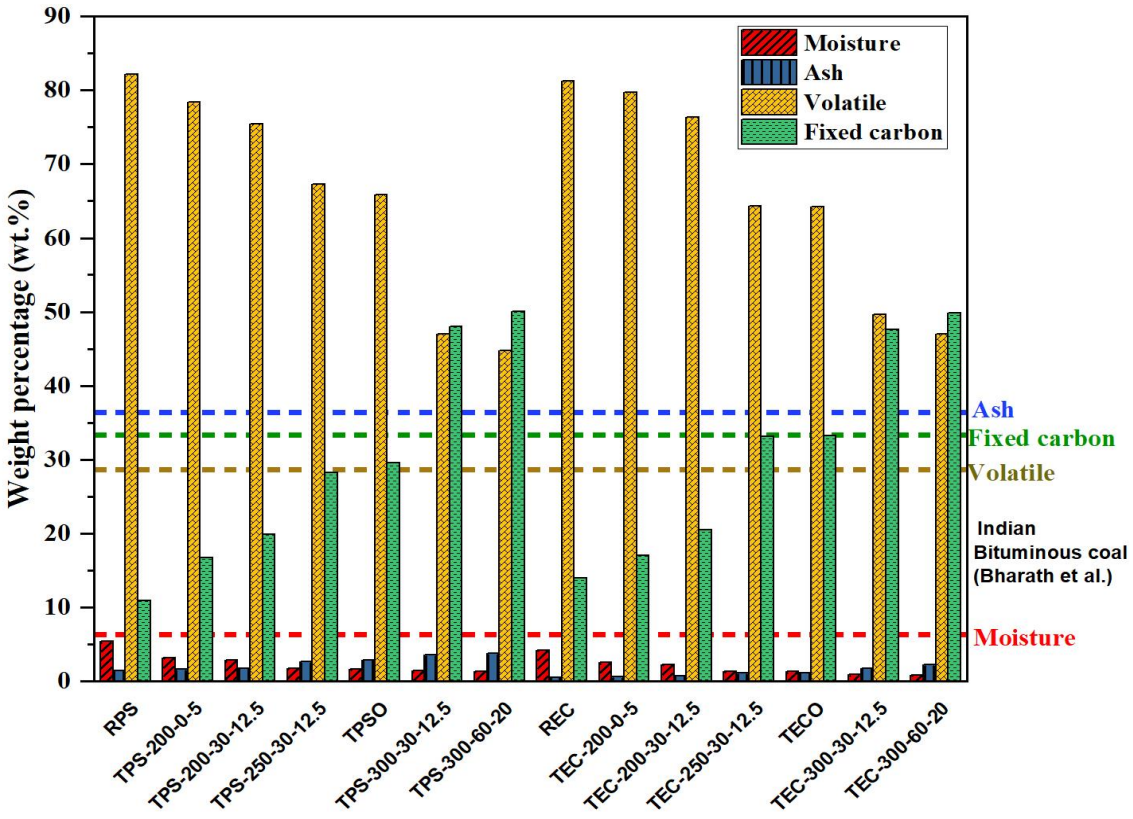

Fig. 4.2 Effect of torrefaction on proximate analysis of pigeon pea stalk and eucalyptus

In the present study, the maximum increase in HHV has been 45.35 % for TPS-300-60-20 and 39.49 % for TEC-300-60-20 as compared to RPS (16.67 MJ/kg) and REC (17.80 MJ/kg), respectively. These results come in agreement with the results reported by C.Buratti et al. (Buratti et al., 2018) and Chen et al. (Chen et al., 2015) where the maximum increase in HHV was 43.3% and 60%, respectively. This increase in HHV

has been probably due to the fact that during torrefaction a major portion of unbound and bound moisture gets removed along with some changes caused in the polymeric structure present in the biomass which reduces lean energy components and low energy chemical bonds such as O-C and H-C (Yang et al., 2015).

Table 4.1 also shows the variation of ash content with varying severity of torrefaction. It can be illustrated from Table 4.1 that with an increase in severity the ash content increases for both torrefied pigeon pea stalk and eucalyptus. Ash content for TPSO and TECO increases to 2.93 and 1.16 wt.%, as compared to RPS (1.49 wt.%) and REC (0.58 wt.%), respectively. This increase in ash content has been due to the fact that during torrefaction, the volatile matters get released, and ash remains intact. It is worth mentioning here that ash content in Indian grade bituminous coal is generally above 35 wt.% such as 36.4 wt% as mentioned by Bharath et al. (Bharath et al., 2018), which is much more as compared to raw and torrefied biomass. Even for the most severe torrefaction the ash content has been 3.76 and 2.24 wt.% for TPS-300-60-20 and TEC-300-60-20, respectively, which is still substantially lesser as compared to coals available in the most part of the world. Seepana et al. (Seepana et al., 2018) in their study for sub-bituminous coal available in India found out that the ash content was as high as 38.39 %.

There is a significant amount of arsenic in the fly ash generated from the usage of coal and arsenic, being extremely hazardous element, leads to some very serious environmental issues especially to aquatic and terrestrial life (Olson et al., 2017; Pandey et al., 2011). On the other hand, ash content in torrefied biomass is on the lower side as compared to medium and lower grade coals (abundant in Indian sub-continent) and using torrefied biomass with coal could significantly reduce ash handling problems

associated with the coal based power plants and thus, reducing its impact on environment. However, proper disposal or utilization of ash from biomass needs to address as it generally contains nitrogen, phosphorus, potassium, sodium, calcium, and other elements which could be very beneficial in production of fertilizers, cement, and road building materials as mentioned by few researchers such as Antonkiewicz et al. (Antonkiewicz et al., 2020), Tosti et al. (Tosti et al., 2020), and Cruz et al. (Cruz et al., 2019).

It can be observed from Table 4.1 and Fig. 4.2 that the fixed carbon of torrefied biomass increases substantially with increase in severity of torrefaction. However for mild torrefaction (200 °C) increase in fixed carbon have been found to be nominal. This has been because at around 200 °C release of volatile matter is nominal and mostly surface moisture gets removed. The fixed carbon of TPSO, TECO, TPS-300-60-20 and TEC-300-60-20 increases by 169.80, 137.38, 356.93 and 256.54 % as compared to their respective raw biomass. Chen et al. (Chen et al., 2011) and M.A. Martin-Lara (Martín-Lara et al., 2017) also reported similar results where fixed carbon for torrefied biomass increased substantially as compared to raw biomass.

Table 4.1 also presents the extent of devolatization with varying operating parameters. There have been 19.84 (TPSO) and 45.47 % (TPS-300-60-20) decrease in the volatile content as compared to RPS while for TECO (20.85 %) and TEC-300-60-20 (42.14 %) also underwent significant decrease in its volatile content as compared to REC. Similar results were obtained by other authors where volatile content decreased substantially for moderate and severe torrefaction (Prins et al., 2006b; Zhang et al., 2018). During torrefaction the moisture content decreased significantly for the torrefied biomass as compared to their corresponding raw biomass. There have been 69.24, 74.58, 67.84 and

78.72 % decrease in moisture content for TPSO, TPS-300-60-20, TECO and TEC-300-60-20. However, the extent of moisture removal has been not prominent with increasing severity of torrefaction, prompting that removal of surface moisture has been more as compared to bound moisture where most of the surface moisture gets removed till mild torrefaction, and hence, the moisture removal after mild torrefaction gets saturated.

4.6 Elemental analysis for raw and torrefied biomass

The effect of torrefaction on the elemental composition of pigeon pea stalk and eucalyptus can be analysed from Table 4.2 and Fig 4.3. Major components of biomass include carbon (C), hydrogen (H), nitrogen (N) and oxygen (O). Carbon and hydrogen are the major sources of energy during combustion. Even though oxygen helps in achieving complete combustion of fuel, but same in larger quantity could significantly reduce the heating value. The Oxygen content has been reduced by 13.1, 21.08, 11.01 and 18.50% for TPSO, TPS-300-60-20, TECO and TEC-300-60-20, respectively, as compared to their respective raw biomass. The impact of torrefaction on oxygen and carbon content has been significant while it has been nominal on hydrogen and nitrogen content. The reduction in oxygen and moisture content have been helpful in the increase of HHV for torrefied biomass. Elemental analysis also reveals that the torrefaction helps in improving the quality of biomass and makes it comparable to the quality of many moderate grade coals available around the world such as carbon and hydrogen content of Indian grade bituminous coal has been 42.4% and 5.3%, respectively which has been similar to the quality of moderate and severely torrefied biomass in the present study (Menon and Patnaikuni, 2017). Similar trend was observed by Martin-Lara et al. (Martín-Lara et al., 2017) where carbon content increased and oxygen content decreased from 45.7 to 53.3% and 46.7 to 38.9% respectively for torrefied oliver tree

pruning at 300 ^{o}C and 60 minutes residence time. Ohliger et al. (Ohliger et al., 2013) also mentioned similar trend, where oxygen content decreased from 43.1 to 33.8% and carbon content increased from 49.8 to 59.4% for torriefied beech wood at 280 ^{o}C and 40 minutes residence time. Torrefied biomass as a co-feed for the boilers can also be beneficial in the significant decrease of NO_X and SO_X (as negligible sulphur content present in biomass) emission from coal based power plants as TPSO and TECO have only 0.8 and 0.6 wt.% of nitrogen content as compared to sub-bituminous coal, which has 2.49% nitrogen content as mentioned by Seepana et al. (Seepana et al., 2018) in their study.

Table. 4.2 Elemental analysis for raw and torrefied biomass

Samples	C (wt.%)	H (wt.%)	N (wt.%)	O (wt.%)	O/C	H/C
RPS	46.1	6.7	0.7	46.5	1	0.15
TPS-200-0-5	48.5	6.8	0.8	43.9	0.9	0.14
TPSO	52.0	6.8	0.8	40.4	0.8	0.13
TPS-300-60-20	55.8	6.7	0.8	36.7	0.7	0.12
REC	48.6	5.6	0.4	45.4	0.93	0.12
TEC-200-0-5	50.6	5.4	0.4	43.6	0.86	0.10
TECO	53.9	5.1	0.6	40.4	0.75	0.09
TEC-300-60-20	57.3	4.9	0.8	37.0	0.65	0.08
Indian coal-1 (Bharath et al., 2018)	43.7	3.8	0.9	14.5	0.33	0.09
Indian coal-2 (Menon and Patnaikuni, 2017)	42.4	3.3	2.5	5.3	0.13	0.08

Fig. 4.3 represents the Van Krevelen diagram and it can be illustrated that torrefaction has been helpful in the improvement of the solid fuel properties of raw biomass and made it comparable to properties of coal available in India. The O/C and H/C ratios have been decreased by 20 and 13.33 %, respectively for TPSO as compared to RPS. This decrease in ratio can be attributed to the removal of CO, CO_2 and H_2O during torrefaction (Prins et al., 2006a). Similar results have been obtained by other

researchers where after torrefaction of biomass, the value of O/C and H/C ratio decreased and in the Van Krevelen diagram the points shifted towards origin after torrefaction (Arias et al., 2008; Bridgeman et al., 2008; Chen et al., 2012; null et al., 2011).

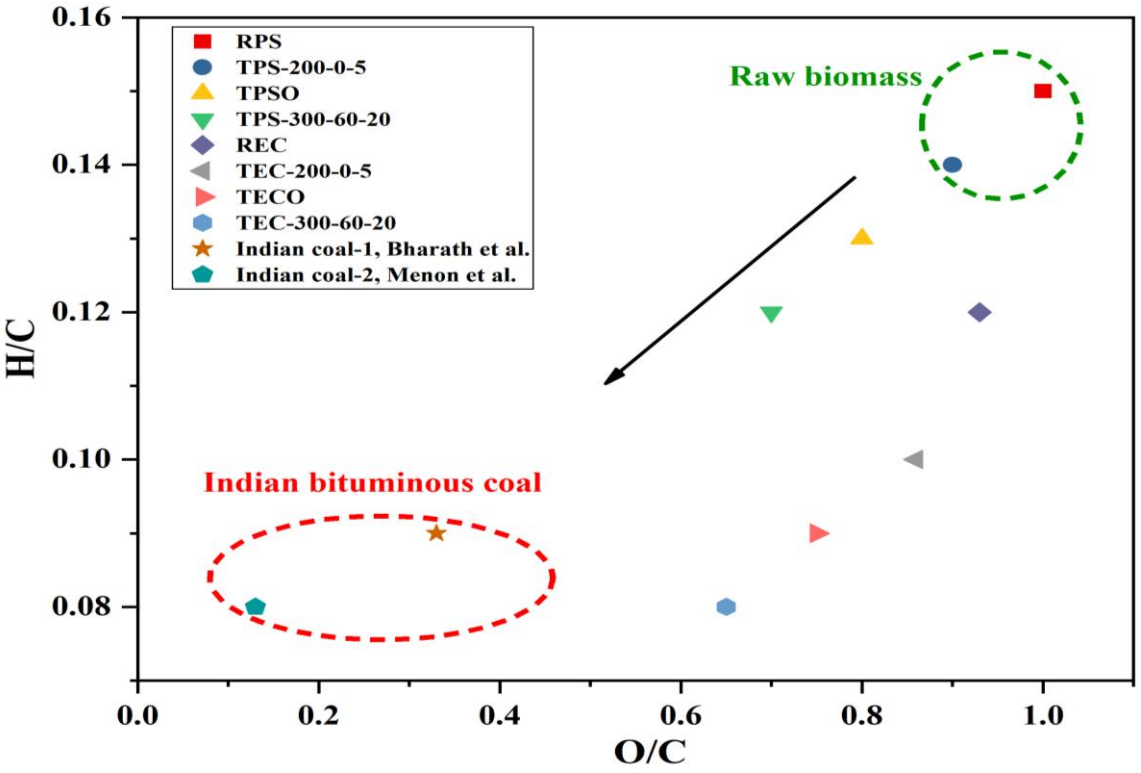

Fig. 4.3 Van Krevelen diagram for raw and torrefied biomass, and Indian coal

4.7 Effect of torrefaction on biomass composition, moisture reabsorption and bulk density

Table 4.3 represents the variation biomass composition of both pigeon pea stalk and eucalyptus with the severity of torrefaction. The hemicellulose content of RPS and REC have been around 24.7, and 21.4 wt.%, respectively, which reduces to 12.1 (TPSO) and 11.4 wt.% (TECO),respectively, confirming that torrefaction even at moderate severity removes substantial amount of hemicellulose from raw biomass. On the other side,

lignin content increases continuously with an increase in the severity of torrefaction, such as for TPS-300-60-20 and TEC-300-60-20 the lignin content has been 44.4 and 48.8 wt.%. This substantial increase in the lignin content of biomass especially for the severe torrefaction condition has been due to major decomposition of hemicellulose along with the partial removal of cellulose while linin does not undergo any decomposition. There has been a partial increase in cellulose content for mild torrefaction, and this has been since at mild torrefaction, only hemicellulose decompose while cellulose and lignin content is maintained in the biomass. However, for moderate and severe torrefaction, the cellulose content decreases with later witnessing major decrease in its cellulose content. A similar trend was observed by Singh et al. (Singh et al., 2020) for torrefaction of Acacia nilotica where cellulose content first increased and then decreased with the severity of torrefaction. There has been no clear trend observed for extractive with the change in torrefaction severity.

Table 4.3 Effect of torrefaction on the fiber analysis of pigeon pea stalk and eucalyptus

Samples	**Fiber analysis (wt.% on dry basis)**			
	Hemicellulose	**cellulose**	**lignin**	**Extractive**
RPS	24.7	48.8	20.6	5.9
TPS-200-0-5	21.9	50.7	20.9	6.5
TPSO	12.1	44.2	36.3	7.4
TPS-300-60-20	9.3	39.5	44.4	6.8
REC	21.4	50.8	26.7	3.1
TEC-200-0-5	18.5	51.4	27.3	2.8
TECO	11.4	45.7	39.8	3.1
TEC-300-60-20	8.2	40.3	48.8	2.7

Biomass tend to reabsorb moisture even after drying. Hence, it becomes important to investigate the moisture reabsorption tendency of biomass to assess its suitability for storage. Also, many researchers have claimed to support that hygroscopic nature of

biomass leads to microbial activity and decomposition when stored for a longer duration (Conag et al., 2017). RPS and REC, when exposed to atmosphere reabsorbs around 25.66 and 21.13 wt.% moisture after 96 hours as compare to its dry weight after being expose to the ambient condition having relative humidity of 56±7 % and at 28.5±4.8 °C. Whereas, under the same condition TPSO and TECO reabsorbs only 3.82 and 3.38 wt.%, respectively.

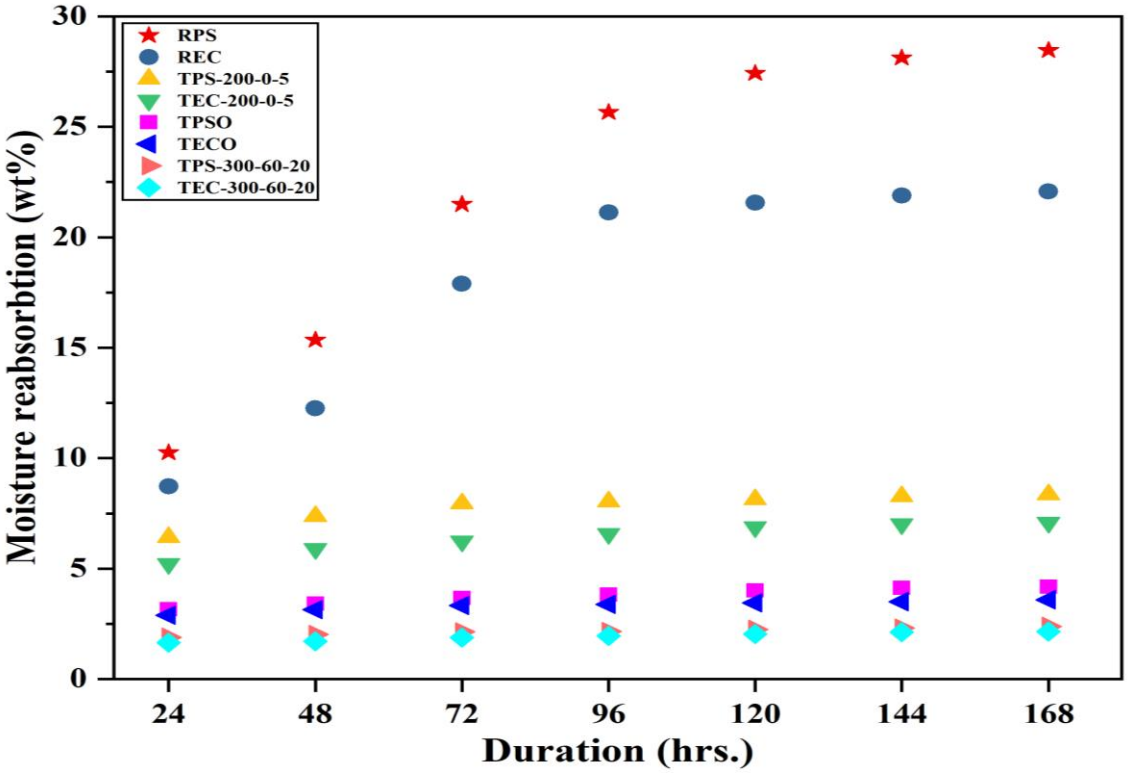

Fig. 4.4 Moisture reabsorption for raw and torrefied biomass over the period of 168 hrs.

The torrefied biomass tend to absorb less moisture as compared to raw biomass owing to the fact that during torrefaction various functional groups are removed which are capable of forming hydrogen bonds with the water (Ohm et al., 2015; Supramono et al., 2015). It can also be observed from Fig. 4.4 that after certain duration of exposer to the atmosphere the moisture reabsorption capability decreases for all the cases, however for RPS and REC the total moisture reabsorption have been still significant as compared to

torrefied biomass. This can be observed by analyzing the data for RPS, REC, TPSO and TECO where moisture reabsorption changed from 25.66 to 28.46, 21.13 to 22.08, 3.82 to 4.18 and 3.38 to 3.59 wt.%, respectively, after 168 hours (T = 26.8±7.3 °C and RH = 61±7.8%) as compared to moisture reabsorbed after 96 hours. Furthermore, these results clearly indicate that as compared to raw biomass torrefied biomass has greater potential to storage for longer periods.

Table 4.1 represents the loose and the tapped bulk density for raw and torrefied biomass (pigeon pea stalk and eucalyptus), where both types of bulk density decreases with an increase in the severity of torrefaction. The bulk density (loose and tapped) decreases because for the torrefied biomass, the porosity of biomass increases with the mass loss which happens with the release of volatiles present in it (Phanphanich and Mani, 2011; Shankar Tumuluru et al., 2011). The loose bulk density for TPSO, TPS-300-60-20, TECO and TEC-300-60-20 decreases by 12.88, 23.72, 11.53 and 18.15 %, respectively, as compared to their corresponding raw biomass. A clear trend can observed from Table 4.1 where both loose and tapped bulk density gradually decreases with the increase in the severity of torrefaction. Rousset et al. (Oliveira Rodrigues, 2009) also observed a similar trend for eucalyptus grandis wood where bulk density decreased by 14.1% as compared to raw biomass for severe torrefaction condition. Based on these observations it would be beneficial to go for the densification of torrefied biomass as this would further reduce the transportation cost (Almeida et al., 2010; Karkania et al., 2012; Martín-Lara et al., 2017). It was further reported by van der Stelt et al. (van der Stelt et al., 2011) that pellets of torrefied biomass as compared to raw biomass pellets showed more desirable hydrophobic behavior and combustion nature.

4.8 Effect of torrefaction on energy density, compaction, flowability and combustibility of biomass

Table. 4.4 Energy density, compactibility, flowability and combustion indices for raw and torrefied biomass (pigeon pea stalk and eucalyptus)

Sample	Energy density (MJ/m^3)	CCI (%)	HR	FR	CI (MJ/kg)	VI (MJ/kg)
RPS	2705.54	32.21	1.48	0.13	142.67	14.86
TPS-200-0-5	2856.36	32.10	1.47	0.21	93.20	14.94
TPS-200-30-12.5	2869.94	33.03	1.49	0.26	77.66	15.02
TPS-250-30-12.5	2934.71	27.17	1.37	0.42	53.31	15.97
TPSO	2953.85	27.23	1.37	0.45	50.46	16.15
TPS-300-30-12.5	3006.59	24.36	1.32	1.02	24.97	15.49
TPS-300-60-20	2999.67	24.33	1.32	1.12	23.26	15.83
REC	4480.26	30.43	1.44	0.17	117.53	15.33
TEC-200-0-5	4586.25	30.35	1.44	0.21	97.49	15.68
TEC-200-30-12.5	4559.86	29.64	1.42	0.27	78.25	15.24
TEC-250-30-12.5	4689.24	28.78	1.40	0.52	44.77	14.88
TECO	4751.78	28.42	1.39	0.52	45.39	15.42
TEC-300-30-12.5	5043.13	28.05	1.39	0.96	27.50	16.11
TEC-300-60-20	5115.23	27.83	1.39	1.06	25.34	16.65

Table 4.4 represents the variation of energy density with varying severity of torrefaction. Energy density increases from 2705.54 to 2953.85, 2705.54 to 2999.67, 4480.26 to 4751.78 and 4480 to 5115.23 MJ/m^3 for TPSO, TPS-300-60-20, TECO and TEC-300-60-20, respectively as compared to their corresponding raw biomass, this indicates that the torrefaction increases the energy density of biomass. As energy density being a function of both HHV and loose bulk density, hence change in energy density for torrefied biomass above 250 ^oC was not significant due to comparable decrease in loose bulk density and increase in HHV. It can also be observed that the

energy density of woody biomass (eucalyptus) tends to be much higher as compared to agricultural residue (pigeon pea stalk) due to much higher bulk density of woody biomass as compared to agricultural residue.

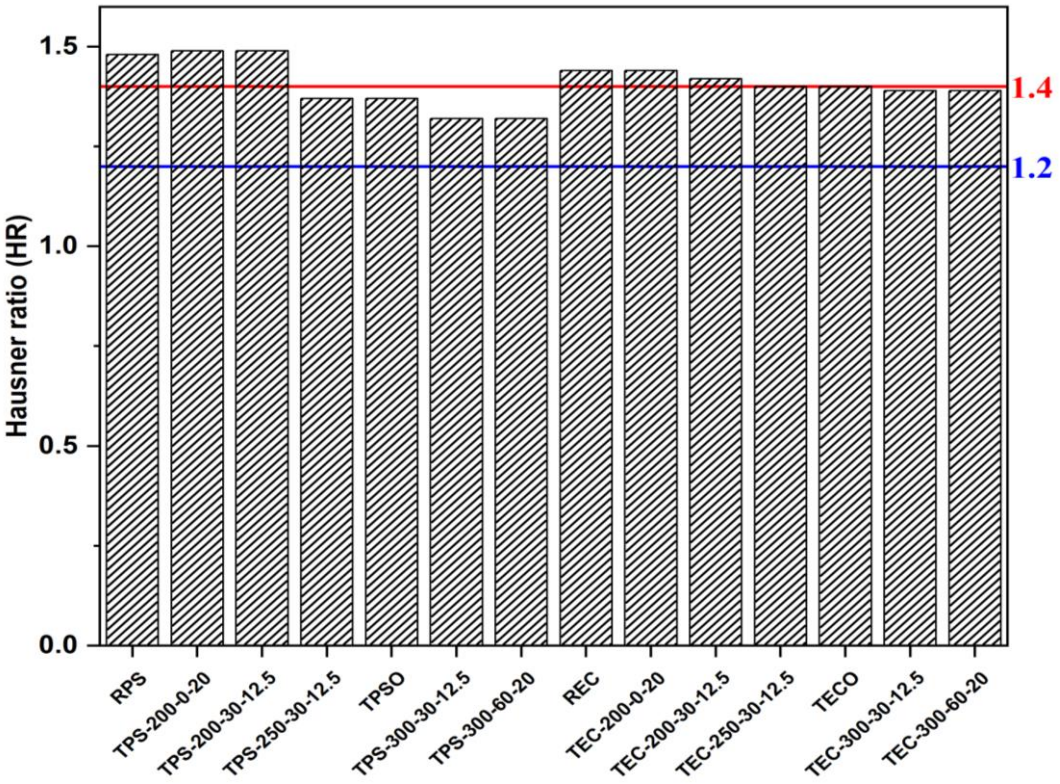

Fig. 4.5 Effect of torrefaction on HR value and its recommended range for fluidized bed reactor.

In order to understand the effect of torrefaction on compaction and flowability of biomass, computation of both CCI and HR have been done. A clear trend can be observed from Table 4.4, where values of both CCI and HR decreases with an increase in the severity of torrefaction. The HR values of biomass in the range of 1.2 to 1.4 have excellent flow properties (Conag et al., 2017). For TPSO and TECO the HR value improved from 1.48 to 1.37 and 1.44 to 1.39, respectively, and falls in the recommended range of operation. In Fig. 4.5 it has been quite obvious that the HR value for both moderate and severely torrefied biomass falls within the desired

operating range which is especially required for the application of fluidized bed reactor. On the other side torrefaction also improves the value of CCI towards the recommended range of 5 to 21 which is considered easy to compact (Tannous et al., 2013), however even after undergoing torrefaction the biomass does not comes within the desired range. It can also be observed from the Table 4.4 that values of compaction has been still on the higher side suggest that compacting raw or torrefied biomass is challenging, and further study needs to be done in this regard.

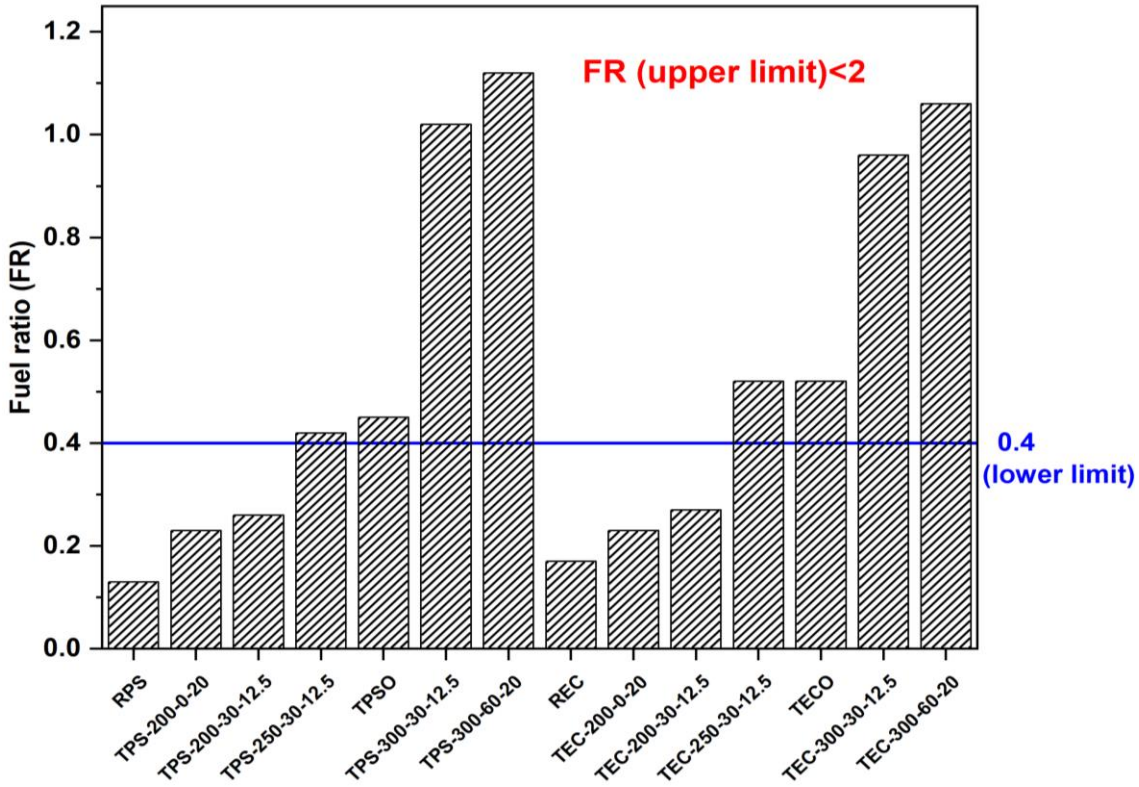

Fig.4.6 Effect of torrefaction on FR value and its recommended range for co-combustion with coal.

.

The solid fuel combustion indices such as FR, VI, and CI play an essential role. Industrial grade coals generally have an FR ranging from 0.4 to 2 (Conag et al., 2018; Ohm et al., 2015). It is essential to mention that raw biomass has a high volatile matter

which results in low value of FR (less than 0.3), which upon combustion gives high smoke and rapid burning with uncontrolled ignition flame (Conag et al., 2018). However, higher FR is also not desirable because this may lead to poor ignition and flame stability (Solihull, 1994). In view of VI, this parameter helps in estimating the gross calorific value of total volatile matter in the solid fuel with an assumption that fixed carbon is entirely made up of carbon. Industrial grade coals with VI greater than 14 MJ/kg is considered desirable (Zaid et al., 2019). In view of mixing alternate solid fuel with coal-based power plants parameter, CI plays a vital role with a desirable range of 20 to 35 MJ/kg (Ohm et al., 2015).

Table 4.4 shows the variation of combustion indices with varying severity of torrefaction for torrefied pigeon pea stalk and eucalyptus. As the severity of torrefaction increases a rapid increment in FR value has been observed. The FR value for TPSO, TPS-300-60-20, TECO and TEC-300-60-20 increases by 246.15, 761.54, 205.88 and 523.53 % as compared to their corresponding raw biomass and these torrefied biomass as a solid fuel for co-combustion with coal in a coal-fired power plants comes in the recommended range of 0.4 to 2.0 (Conag et al., 2017; Ohm et al., 2015).

The CI value for RPS and REC have been 142.62 and 117.53 MJ/kg, respectively, which has been way above the desired limit thus making it non-ideal for co-combustion with coal. The high value of CI results due to the lower value of FR which is inversely proportional to CI and the low value of FR results from high volatile content which is again not desirable for co-combustion with coal. Also, for torrefied biomass percentage change in FR value has been much higher as compared to the percentage change in HHV_{db} (directly proportional to CI), making FR more significant term for variation of CI value. On analyzing Table 4.4 it can be observed that CI value decreases sharply for

torrefied biomass, and for TPSO, TPS-300-60-20, TECO and TEC-300-60-20 it drops to 50.46, 23.26, 45.39 and 25.34 MJ/kg. The decrease in CI value is indicative of torrefaction, improving the compatibility of biomass for co-combustion with coal. However, on analyzing the CI value in Fig. 4.7, it can be clearly observed that only severely torrefied biomass comes within the desired range of CI value recommended for co-combustion with coal. It can also be illustrated from Table 4.4 that VI does not follow any particular trend towards change in severity of torrefaction. However, in the present study most of the torrefied biomass falls within the recommended value for VI (above 14 MJ/kg) (N Magasiner 2001).

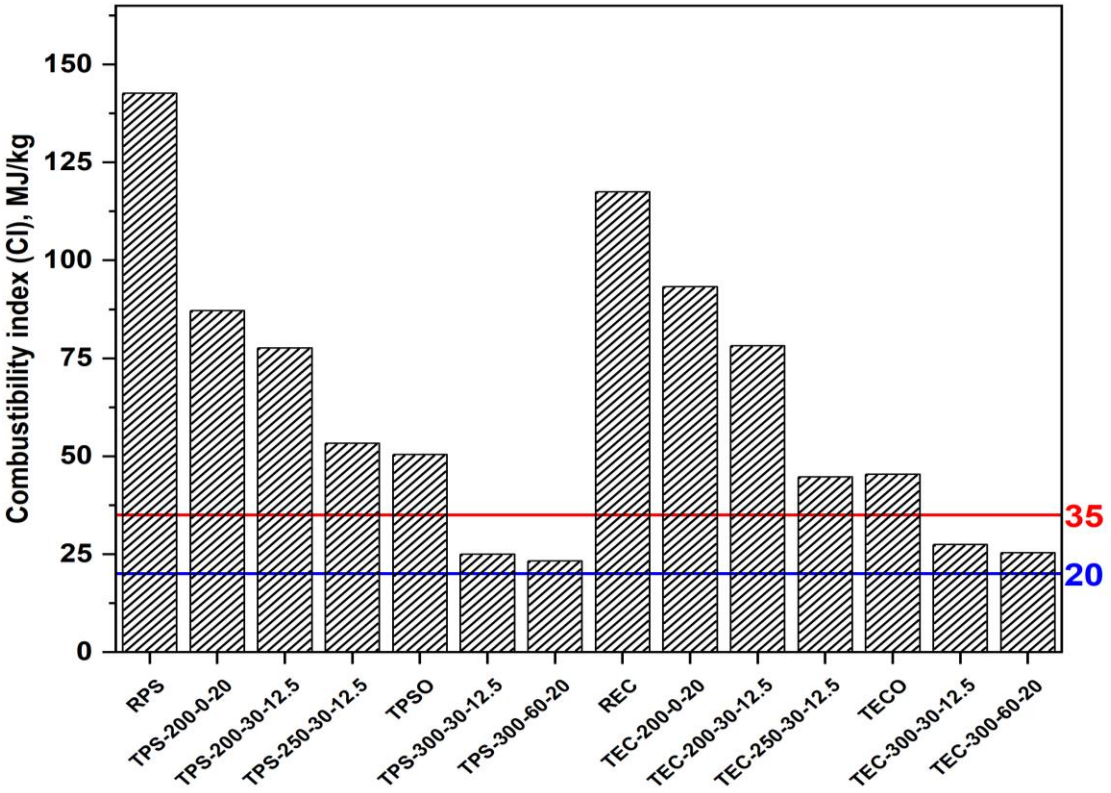

Fig.4.7 Effect of torrefaction on CI value and its recommended range for co-combustion with coal.

4.9 Effect of torrefaction on FTIR analysis of pigeon pea stalk and eucalyptus

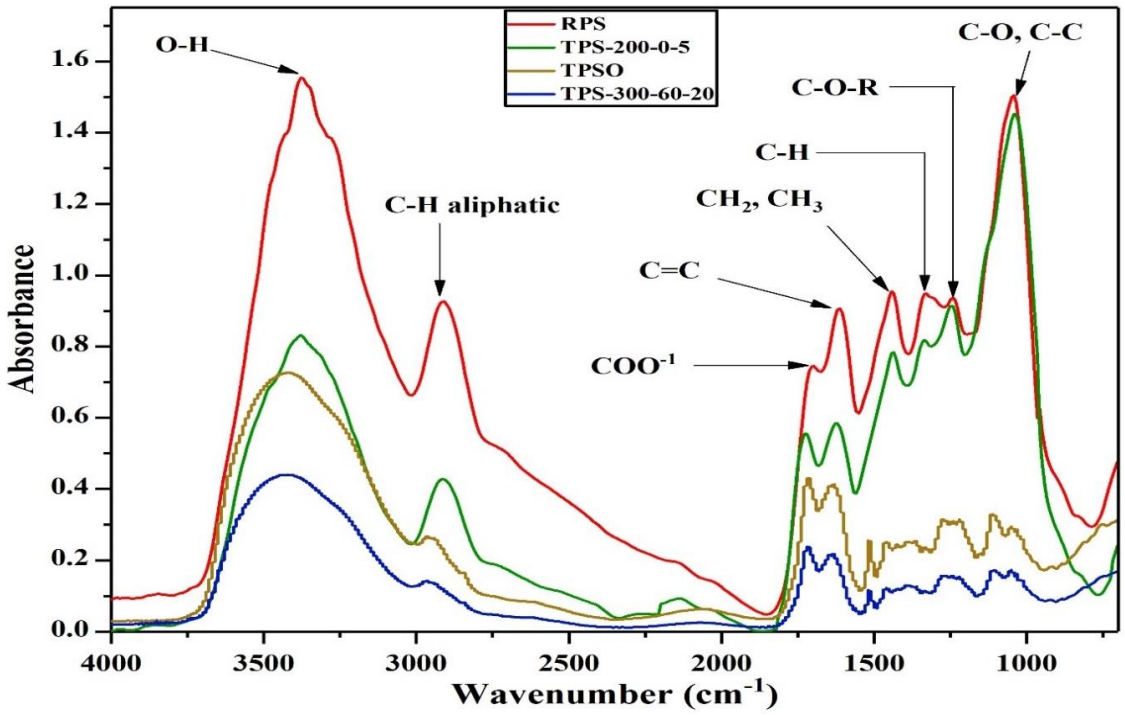

Fig. 4.8 Infrared spectra of raw and torrefied pigeon pea stalk.

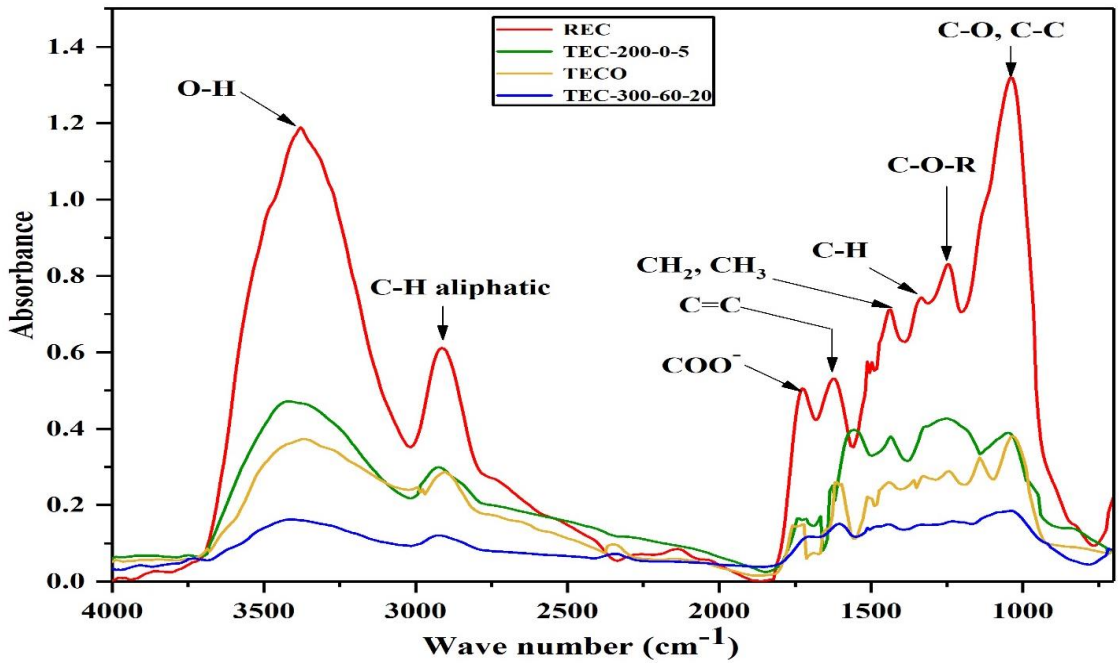

Fig. 4.9 Infrared spectra of raw and torrefied eucalyptus.

Figs. 4.8, and 4.9 represents the infrared (IR) spectra for pigeon pea stalk and eucalyptus, respectively, and Table 4.5 presents the position of significant peaks in their corresponding samples along with the identification groups. Based on inferences made from Figs. 4.8 and 4.9, it can be observed that both the biomass contains many oxygen containing functional groups. However, the vibration intensities of these functional groups gradually decrease with an increase in severity of torrefaction with the substantial decrease being observed for optimum and severe torrefaction conditions.

The decrease in intensity of O-H (3322-3398 cm^{-1}) absorption peak results due to the dehydration reaction followed with the degradation of hemicellulose and cellulose (Sadaka and Negi, 2009). The broader O-H band has been be due to the presence of inter and intra molecular hydrogen bonds present in the crystalline hemicellulose and cellulose. The presence of C-H peak (2891-2928 cm^{-1}) gives the indication for the presence of methyl and methylene groups in biomass. However, the intensity of C-H band diminishes with severe torrefaction suggesting that the removal of such groups happens during torrefaction. The presence of acetyl groups in hemicellulose and cellulose can be represented by the absorption peak of COO^- (1639-1679 cm^{-1}). The absorbance bands in the range of 1595-1620 cm^{-1} represents the C=C stretching vibrations indicating the presence of aromatic groups in both the biomass. However, decreased intensity of absorbance confirms the removal or the breakdown of such groups during torrefaction.

CH_2 scissoring vibration and CH_3 asymmetric stretching have been represented with the absorbance bands in the range of 1416 to 1454 cm^{-1}, and other peaks like C-O-R (1217-1231 cm^{-1}), alcoholic C-O and C-C (1019-1112 cm^{-1}) also show diminishing absorbance intensity with the severity of torrefaction, which can be attributed to

carbohydrate degradation present in cellulose. The degradation of carbohydrates occurs mainly due to decarboxylation and dehydration reactions during the torrefaction process (Chen et al., 2011). These results confirm the structural changes during torrefaction for hemicellulose and cellulose with diminishing peak intensity for oxygen containing functional groups.

Table 4.5 Position vibration, in cm^{-1}, of the most representative peaks found in the infrared analysis of raw and torrefied biomass (pigeon pea stalk and eucalyptus).

FUNCTIONAL GROUP	RPS	TPS-200-0-5	TPSO	TPS-300-60-20	REC	TEC-200-0-5	TECO	TEC-300-60-20
O–H in polymer compounds	3362	3368	3375	3375	3396	3349	3328	3384
C–H aliphatic symmetrical	2891	2883	2907	2912	2927	2891	2914	2922
COO-	1680	1727	1732	1750	1641	1675	1653	1677
Aromatic C = C skeletal vibration	1605	1617	1609	1614	1610	1619	1597	1605
CH_2 scissoring vibration, assymetric CH_3 stretching vibration	1424	1427	1468	1470	1418	1436	1446	1452
C-H bending vibration	1311	1303	1318	1327	1307	1335	1324	1312
C-O-R	1225	1243	1214	1227	1228	1223	1211	1238
C-O and C-C stretching vibration of alcoholic group	1032	1090	1081	1105	1093	1085	1073	1084

4.10 Effect of torrefaction on morphology of pigeon pea stalk and eucalyptus

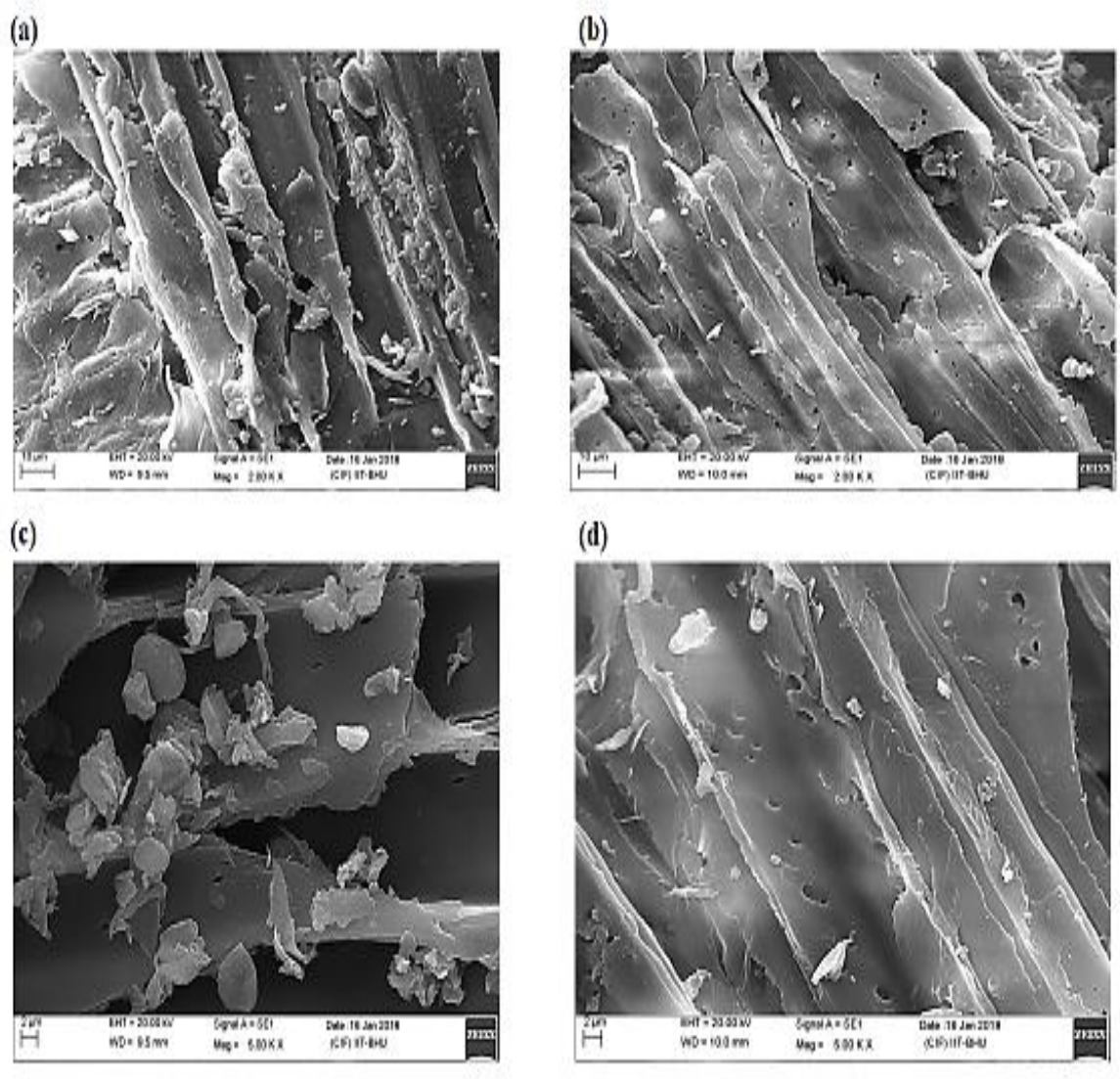

Fig. 4.10 SEM images of (a) RPS (2000X), (b) TPSO (2000X), (c) RPS (5000X) and (d) TPSO (5000X).

Figs. 4.10 ((a) and (b)) and 4.11 ((a) and (b)) represents the SEM micrographs for pigeon pea stalk (RPS and TPSO) and eucalyptus (REC and TECO), respectively, at 2000X magnification, and similarly Figs. 4.10 ((b) and (c)) and 4.11 ((b) and (c)) represents the same at 5000X magnification. On comparison of the SEM images for raw and torrefied biomass, it has been quite clear that significant changes occurred on the

morphology of RPS and REC after undergoing torrefaction at their respective optimum condition.

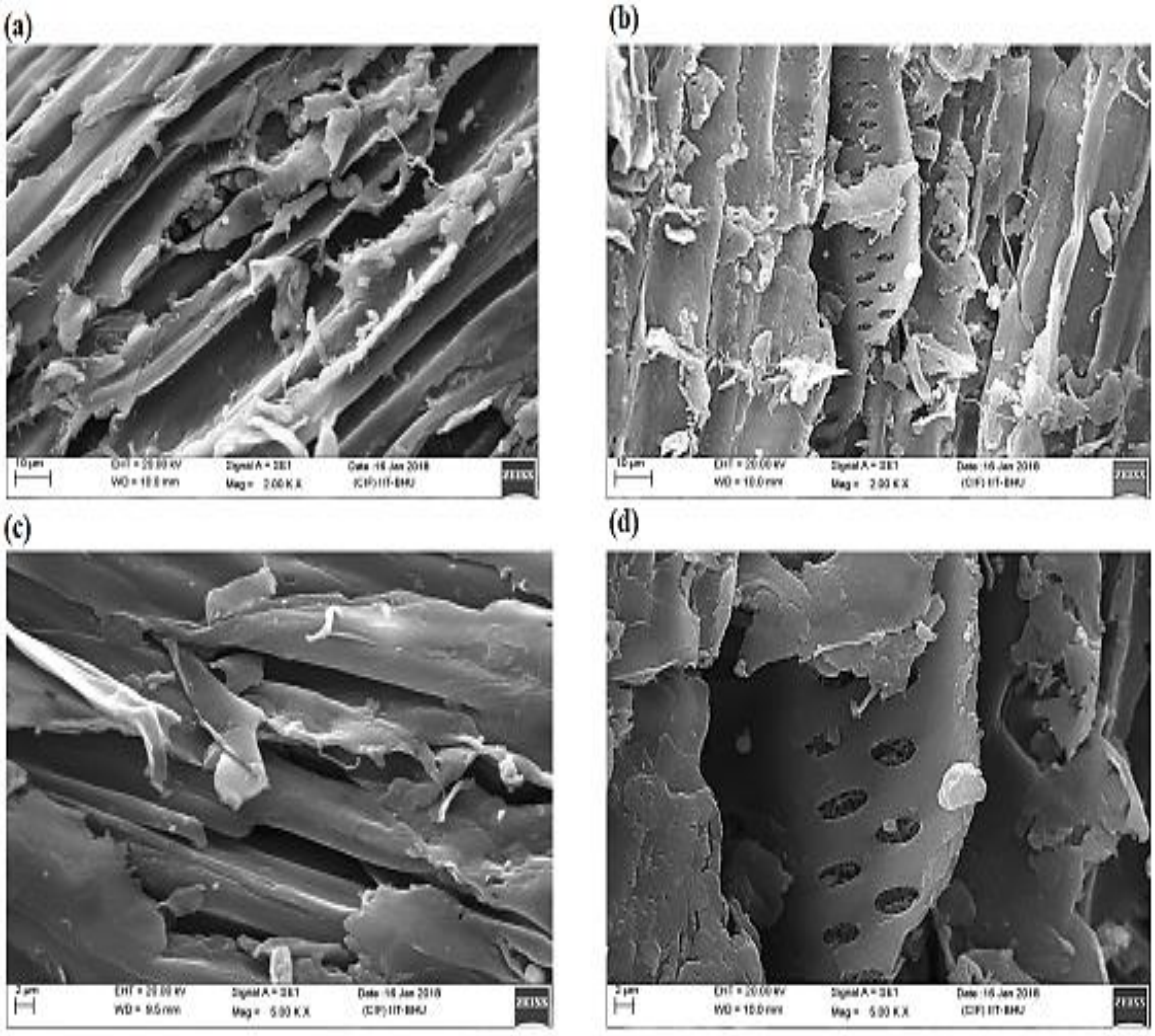

Fig. 4.11 SEM images of (a) REC (2000X), (b) TECO (2000X), (c) REC (5000X) and TECO (5000X).

In Figs. 4.10 ((b), (d)) and 4.11 ((b), (d)) for TPS and TECO, respectively, quite a few number of pores and cracks have been generated. The generation of porosity contributes to the decrease in bulk density and cracks decrease the structural strength of the biomass. The generation of pores and cracks can be related to the fact that hemicellulose decomposes during torrefaction with the release of methoxyl groups

(Uemura et al., 2015). The increased porosity helps in improving the gasification and combustion characteristics of torrefied biomass through the facilitation of reactants and products into the carbon matrix (Niu et al., 2019a). Hemicellulose being the binder in the structure of biomass, suggests that torrefaction also brings significant structural changes in the biomass. Also for the torrefied biomass at the optimum condition as given in Figs. 4.10 ((b), (d)) and 4.11 ((b), (d)), there have been few breakdowns along the filaments of the biomass, which makes it brittle (Niu et al., 2019b). This decrease in structural strength could result in a reduction of power consumption required during the crushing and compacting of biomass. Similar observations were made by other researchers for torrefied biomass under similar conditions (Almeida et al., 2010; Martín-Lara et al., 2017; Oliveira Rodrigues, 2009; Shankar Tumuluru et al., 2011).

4.11 Thermogravimetric analysis of raw and torrefied biomass

(a)

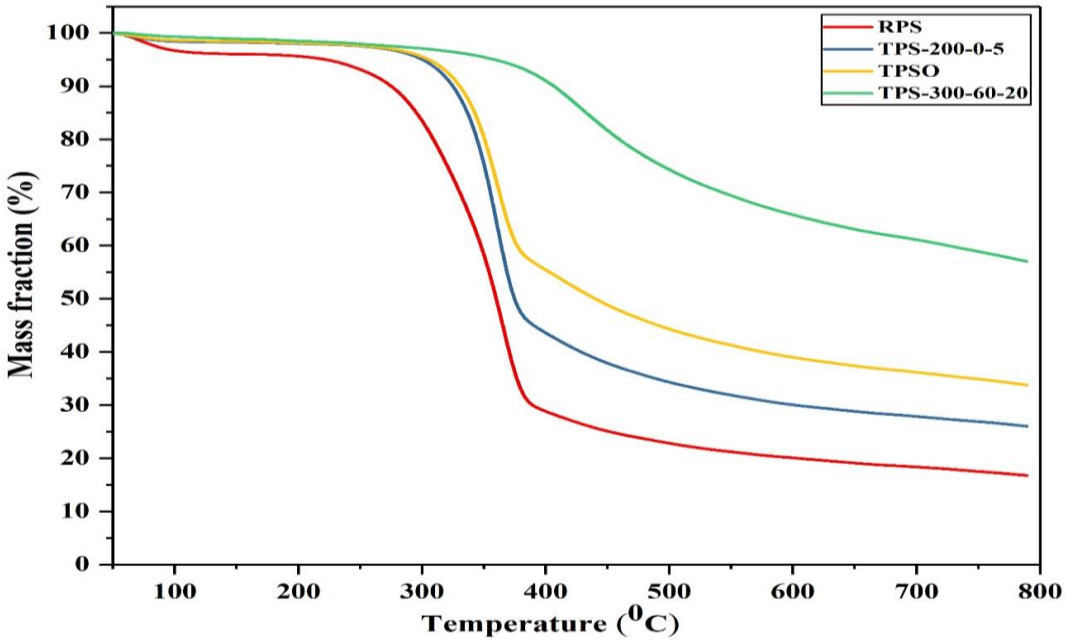

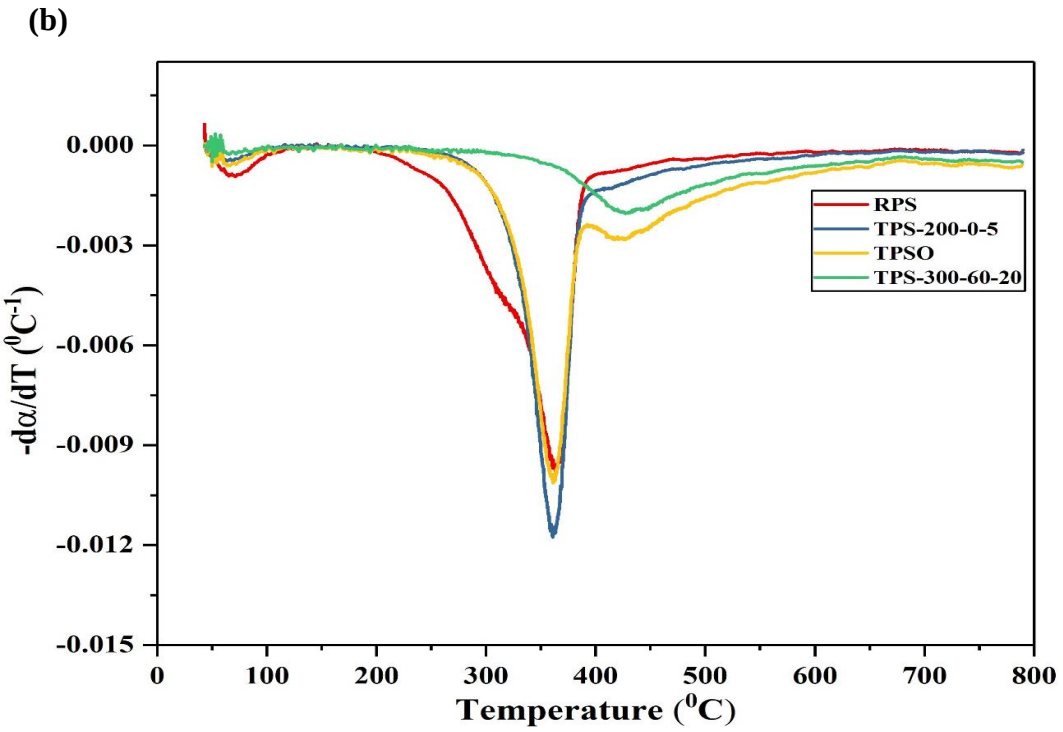

Fig. 4.12 Experimental curves of, (a) TGA, (b) DTG for raw and torrefied pigeon pea stalk.

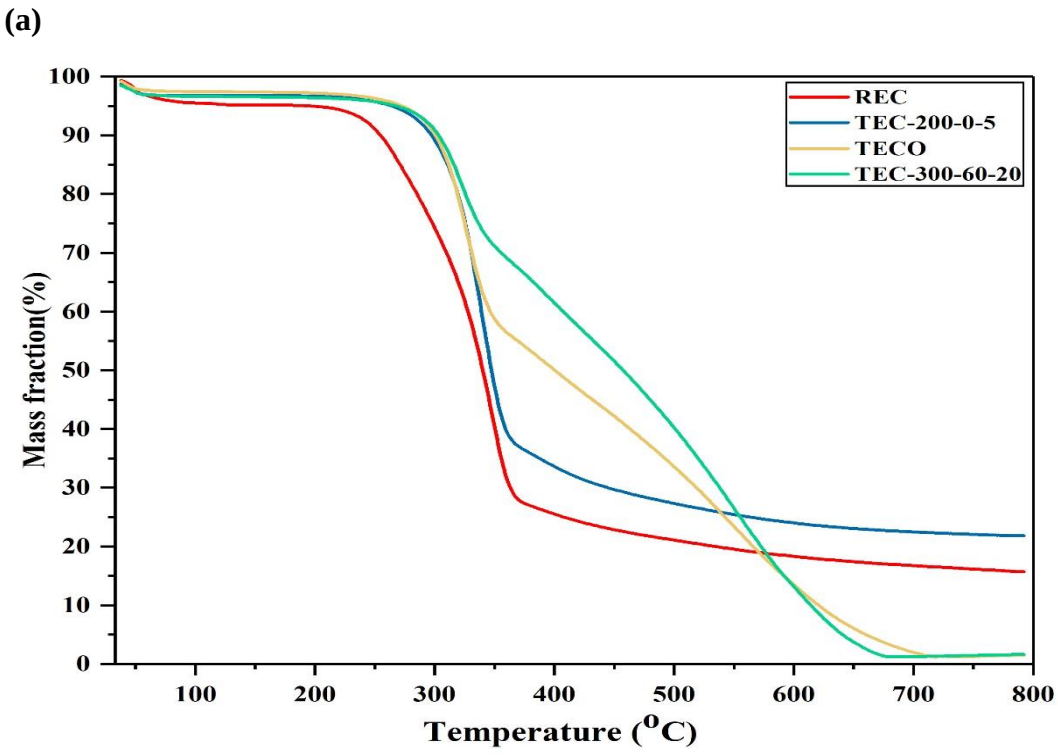

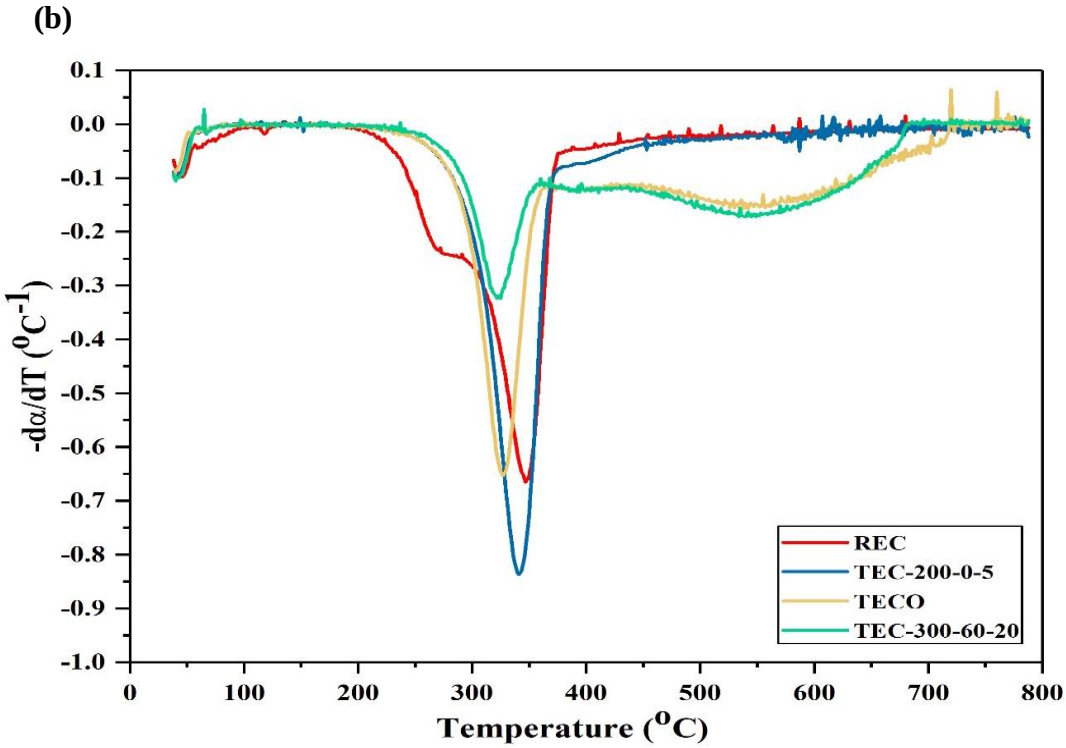

Fig. 4.13 Experimental curves of, (a) TGA, (b) DTG for raw and torrefied eucalyptus.

TGA and DTG analysis have been done to study the thermal decomposition of raw and torrefied biomass during pyrolysis. Thermal decomposition of hemicellulose, cellulose, and lignin happens in the temperature range of 150-350, 275-350 and 250-500 °C, respectively (Patrick C.A. Bergman 2005). There have been distinct stages of weight loss, as observed in Figs. 4.12 (b) and 4.13 (b) for raw and torrefied biomass (pigeon pea stalk and eucalyptus). The first stage can be presented till 150 °C corresponded to the loss of surface moisture and absorbed or equilibrium moisture. However, only RPS and REC shows the significant moisture loss (first stage) as compared to torrefied biomass which completely disappears for severe torrefaction condition (TPS-300-60-20 and TEC-300-60-20), which confirms the removal of surface and absorbed moisture during torrefaction. Martine-Lara M.A. et al. (Martín-Lara et al., 2017) also mentioned

similar explanation for moisture loss for olive tree pruning which underwent torrefaction.

The next stage in TGA and DTG curves corresponds to hemicellulose decomposition in the temperature range of 175ºC to 315ºC. The shoulder shaped curve present in DTG corresponds to hemicellulose decomposition during thermal decomposition, and it completely disappears for TPS-300-60-20 and TEC-300-60-20, confirming significant decomposition of hemicellulose during torrefaction.

The Third stage has been observed between 300ºC to 385ºC which corresponds to cellulose decomposition. In the DTG curve (Figs. 4.12 (b) and 4.13 (b)), the peak corresponding to cellulose decomposition shows an increase in the intensity for TPS-200-0-5 and TEC-200-0-5 as compared to RPS and REC, respectively, suggesting that the thermal stability of cellulose during mild torrefaction decreases. A similar trend was observed for Norway spruce where the intensity of peak corresponding to cellulose decomposition during mild and severe torrefaction increased and decreased, respectively, as compared to raw biomass (Bach et al., 2017). The intensity of peak corresponding to cellulose decomposition decreased significantly for TPS-300-60-20 and TEC-300-60-20, due to the loss of cellulose for the most severely torrefied biomass.

In Figs. 4.12 (b) and 4.13 (b), between 450 to 650ºC smaller peaks can be observed for TPSO, TECO, TPS-300-60-20 and TEC-300-60-20, suggesting that moderate and severe torrefaction decreases the thermal stability of lignin present in biomass, however the intensity of smaller peaks have been more prominent for torrefied eucalyptus. Martine-Lara M.A. et al. (Martín-Lara et al., 2017)also mentioned a decrease in thermal stability of lignin due to the torrefaction of biomass. Based on TGA and DTG analysis,

pyrolysis in the moderate temperature range (400-600 ^{o}C) might be suitable for moderately torrefied pigeon pea stalk and eucalyptus at their respective optimum condition. On the other side, due to significant decrease in the thermal stability of lignin especially for severe torrefied eucalyptus, high temperature (above 600 ^{o}C) pyrolysis might be suitable.

4.12 Effect of torrefaction on kinetic parameters for the pyrolysis of raw and torrefied biomass

In the present study, the activation energy has been calculated using the direct Arrhenius plot method. At different values of n, the data obtained have been fitted, and the best-fitted regression line with the highest value for correlation coefficient R^2 has been chosen. Arrhenius Plots corresponding to three different pseudo-components have been presented in Figs. (4.14)-(4.16) and Figs. (4.17)-(4.19) for pigeon pea stalk and eucalyptus, respectively. It can be observed from Table 4.6 and 4.7 that mild severity torrefaction has little effect on activation energy of pseudo-components for RPS, REC, TPS-200-0-5 and TEC-200-0-5. This behavior is similar to other reported studies on pyrolysis kinetics of biomass (Broström et al., 2012; Tapasvi et al., 2013). Activation energy of hemicellulose for pigeon pea stalk has been decreased from 88.20 to 66.97 and 49.57 (kJ/mol) for TPSO and TPS-300-60-20 as compared to RPS. However, it can also be observed from Table 4.7 that for the eucalyptus biomass, the effect of torrefaction on the activation energy of hemicellulose has not been significant.

Torrefaction at the most severe condition has the significant effect on activation energy of cellulose present in both the biomass. The value of activation energy for cellulose dropped from 111.26 to 79.83 and 264.49 to 218.10 (kJ/mol), for TPS-300-60-20 and TEC-300-60-20, respectively, as compared to raw their corresponding raw biomass

(RPS and REC). This indicates that the thermal stability of cellulose decrease significantly for severe torrefaction of biomass.

In the case of eucalyptus, the thermal stability of lignin decreases due to the decrease in the value of its activation energy from 48.05 to 32.20 and 24.92 kJ/mol (32.99 and 48.14% drop) for TECO and TEC-300-60-20, respectively, as compared to REC. A similar trend was observed by Martine-Lara M.A. et al. (Martín-Lara et al., 2017), where the activation energy of lignin for olive tree decreased due to torrefaction of biomass. However, in the case of pigeon pea stalk, torrefaction has nominal or no effect on the activation energy of lignin.

On analyzing Tables 4.6 and 4.7 it can be observed that the contribution factor (C_H) of hemicellulose for decreased substantially, resulting due to lesser hemicellulose concentration in torrefied biomass. These results for the contribution factors have been in agreement with those reported in other literature in the field of biomass torrefaction (Amutio et al., 2012; Bach et al., 2014; Martín-Lara et al., 2016). But in the case of TPS-200-0-5 and TEC-200-0-5 for cellulose decomposition its contribution factor (C_C) slightly increases due to a decrease in its thermal stability while at the same time cellulose not getting thermally decompose at mild torrefaction.

The contribution factor for lignin (C_L) increases significantly for moderately and severely torrefied eucalyptus due to major decomposition of hemicellulose, thus, making biomass rich in lignin. It can be illustrated from Table 4.6 and 4.7 that mild torrefaction (TPS-200-0-5 and TEC-200-0-5) has little or no effect on the value of total or overall activation energy. However, with increase in the severity of torrefaction decreases the value of total activation energy significantly by 16.99, 44.97, 36.11 and

54.38 %, for TPSO, TPS-300-60-20, TECO and TEC-300-60-20, respectively as compared to their corresponding raw biomass.

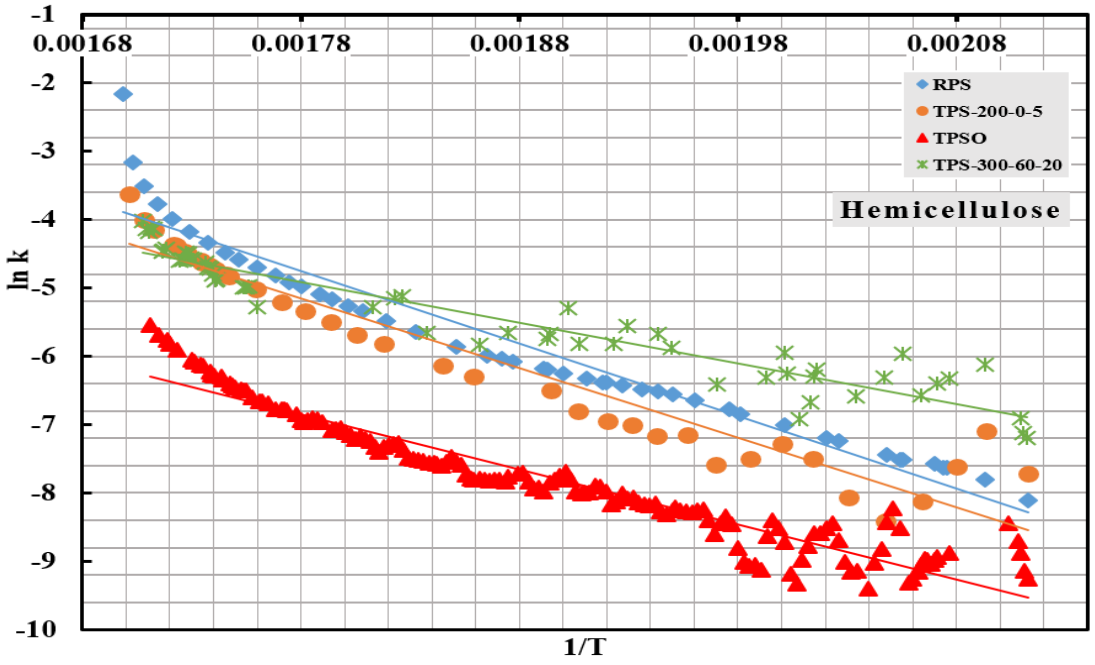

Fig. 4.14 Plot obtained by Arrhenius method for hemicellulose present in pigeon pea stalk.

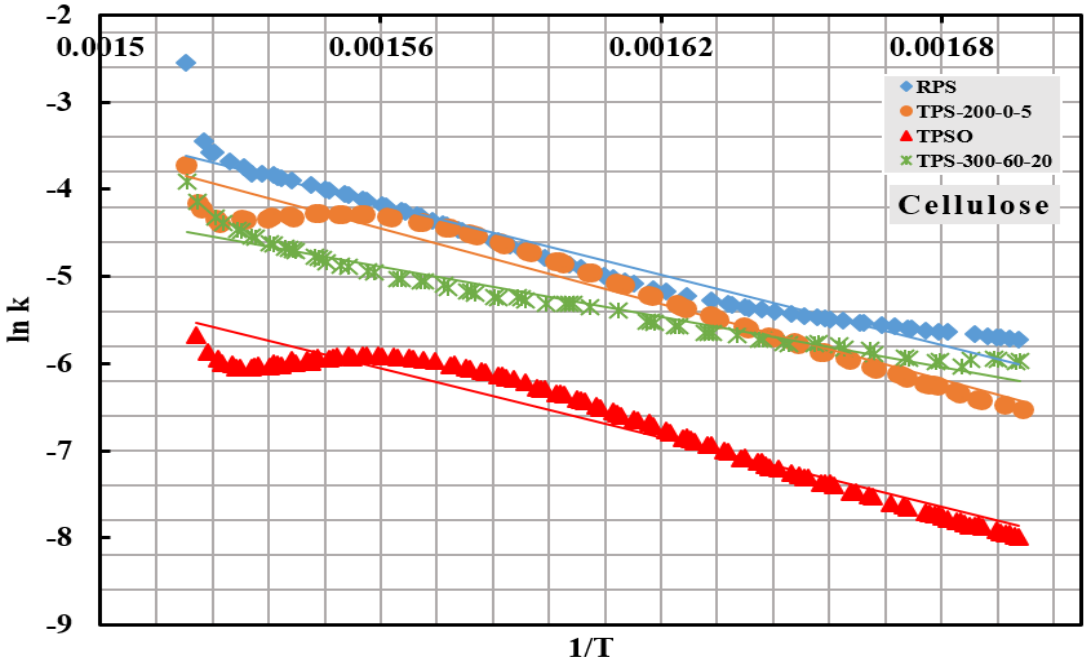

Fig. 4.15 Plot obtained by Arrhenius method for cellulose present in pigeon pea stalk.

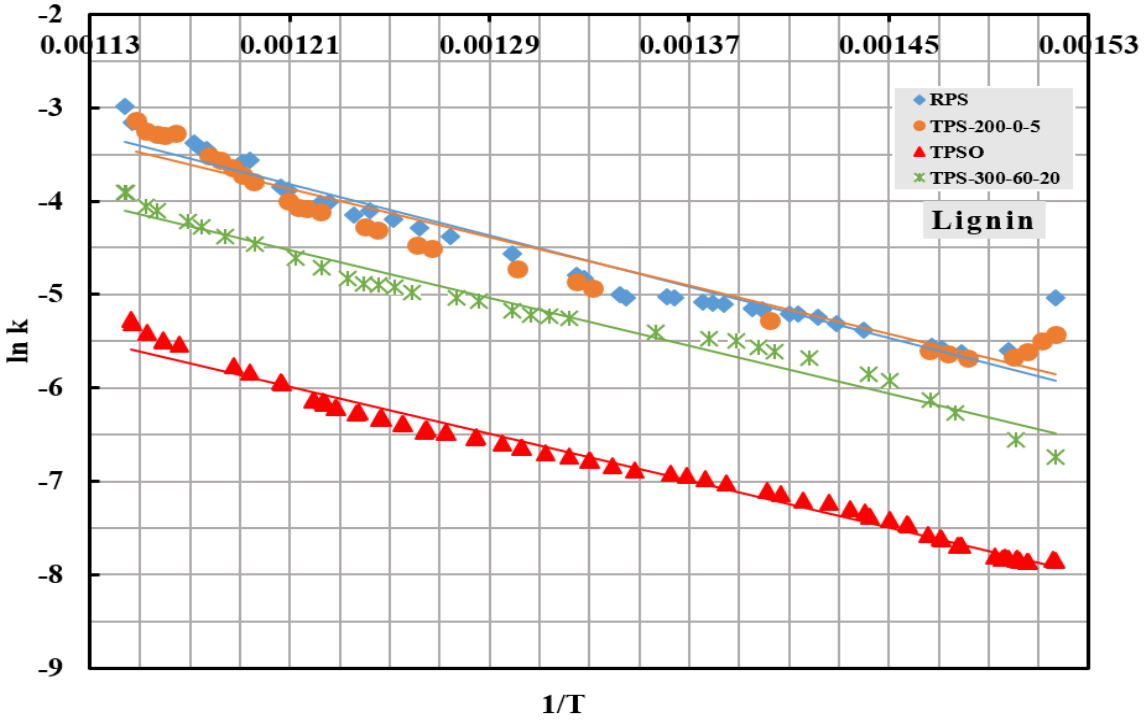

Fig. 4.16 Plot obtained by Arrhenius method for lignin present in pigeon pea stalk.

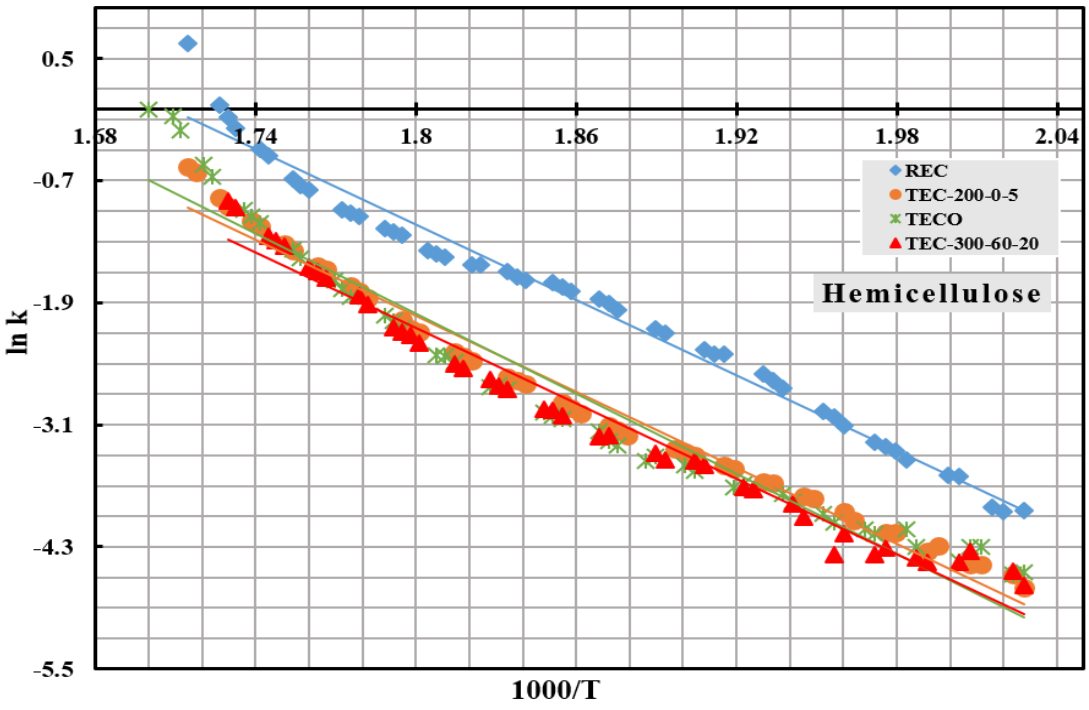

Fig. 4.17 Plot obtained by Arrhenius method for hemicellulose present in eucalyptus.

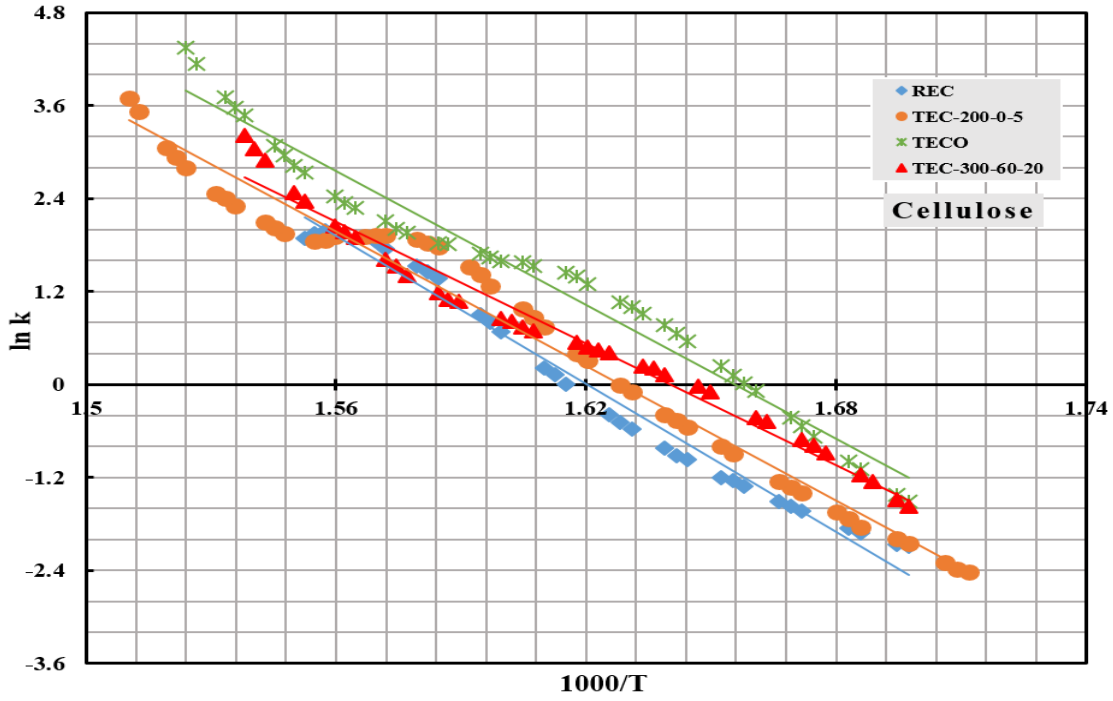

Fig. 4.18 Plot obtained by Arrhenius method for cellulose present in eucalyptus.

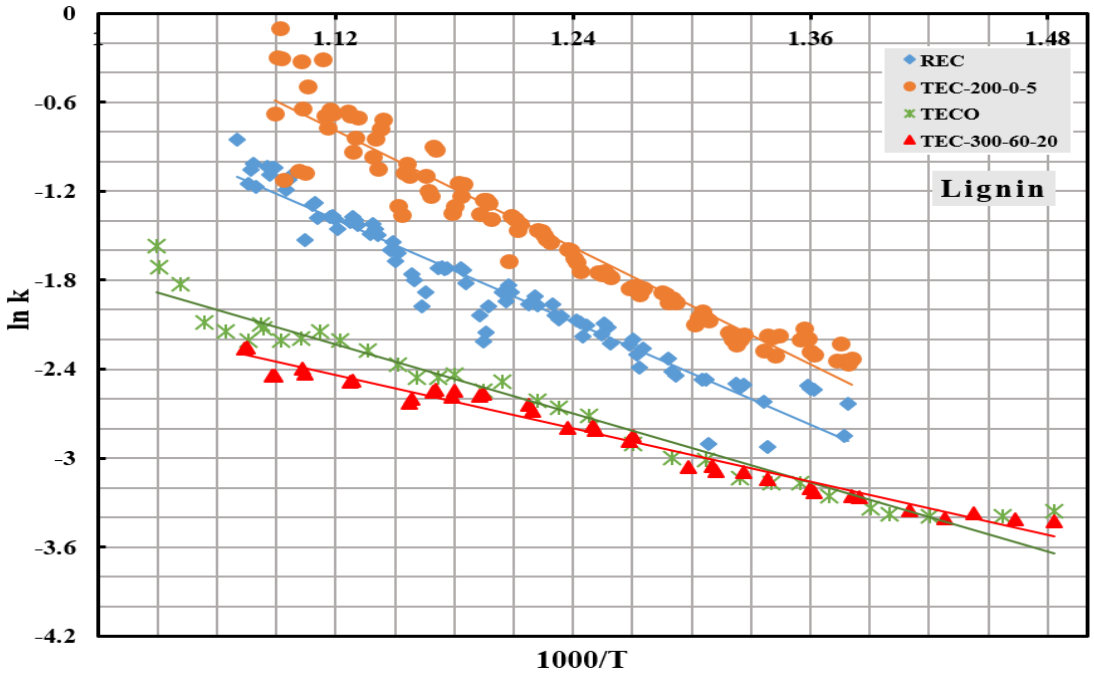

Fig. 4.19 Plot obtained by Arrhenius method for lignin present in eucalyptus.

Table. 4.6 Kinetic parameters for the pseudo-components of raw and torrefied pigeon pea stalk

Kinetic parameters	RPS	TPS-200-0-5	TPSO	TPS-300-60-20
E_H(kJ/mol)	88.20	84.46	66.97	49.57
ln A_H	14.13	12.92	7.49	5.70
n_H	0.55	0.22	0.40	0.45
R^2_H	0.93	0.93	0.91	0.91
C_H	0.24	0.08	0.07	0.05
Linear correlation equation for hemicellulose (ln k vs 1/T)	Y= -10609X + 14.13	Y= -10159X + 12.92	Y= -8054.9X + 7.49	Y= -5962.7X + 5.70
E_C(kJ/mol)	111.26	120.01	110.05	79.83
ln A_C	16.70	18.06	14.59	10.09
n_C	0.59	0.40	0.43	0.16
R^2_C	0.94	0.96	0.94	0.95
C_C	0.61	0.68	0.48	0.11
Linear correlation equation for cellulose (ln k vs 1/T)	Y= -13383X + 16.70	Y= -14435X + 18.06	Y= -13237X + 14.59	Y= -9602.3X + 10.09
E_L(kJ/mol)	57.03	53.64	52.26	53.13
ln A_L	4.48	3.93	1.62	3.20
n_L	2.30	2.10	1.9	1.80
R^2_L	0.93	0.93	0.98	0.97
C_L	0.15	0.24	0.45	0.79
Linear correlation equation for lignin (ln k vs 1/T)	Y= -6860.5X + 4.48	Y= -6452.5X + 3.93	Y= -6285.3 + 1.62	Y= -6391.4 + 3.20
Over all activation energy (E_T), KJ/mol	97.62	101.22	81.03	53.72

Where Y= ln k and X= 1/T and for subscript (H: Hemicellulose, C: Cellulose and L: Lignin)

Table. 4.7 Kinetic parameters for the pseudo-components of raw and torrefied eucalyptus

Kinetic parameters	REC	TEC-200-0-5	TECO	TEC-300-60-20
E_H (kJ/mol)	102.52	103.62	109.17	102.52
ln A_H	21.06	20.41	21.63	20.04
n_H	1	0.32	0.4	0.3
C_H	0.34	0.17	0.15	0.11
R^2_H	0.98	0.98	0.95	0.97

Linear correlation equation for hemicellulose (ln k vs 1/T)	Y=-12.33X + 21.06	Y=-12.46X + 20.41	Y=-13.31X + 21.63	Y=-12.33X + 20.04
E_C (kJ/mol)	264.49	240.86	240.06	218.10
ln A_C	51.54	47.17	47.80	43.02
n_C	1.8	2	3	3.5
C_C	0.52	0.65	0.34	0.25
R^2_C	0.98	0.98	0.97	0.98
Linear correlation equation for cellulose (ln k vs 1/T)	Y=-31.81X + 51.54	Y=-28.97X + 47.17	Y=-28.87X + 47.80	Y=-26.23X +43.02
E_L (kJ/mol)	48.05	54.61	32.20	24.92
ln A_L	5.08	6.57	2.10	0.92
n_L	1.5	1.8	0.7	0.43
C_L	0.14	0.18	0.51	0.64
R^2_L	0.93	0.93	0.96	0.97
Linear correlation equation for lignin (ln k vs 1/T)	Y=-5.78X + 5.08	Y=-6.56X + 6.57	Y=-3.87X +2.10	Y=-2.99X +0.92
Overall activation energy, E_T (kJ/mol)	179.10	183.98	114.41	81.73

Where Y= ln k and X= 1/T and for subscript (H: Hemicellulose, C: Cellulose and L: Lignin)

4.13 Characteristics of liquid product (condensable gases) obtained during the torrefaction of biomass

The liquid product obtained after torrefaction of pigeon pea stalk and eucalyptus contain a large amount of water in it. TPSO and TECO contains 66.3 and 63.6 wt.% of the water in its liquid part obtained after their torrefaction. Water content in the liquid product has been obtain from the biomass itself due to the dehydration reaction (Chen et al., 2018b; Yue et al., 2017) and thermal degradation of organic components, mainly hemicellulose. In the case of mild (TPS-200-0-5 and TEC-200-0-5) and severe (TPS-300-60-20 and TEC-300-60-20) torrefaction, the water content has been in the range of 80-85 and 50-56 wt.%, respectively. It can be observe that with increasing the severity of torrefaction, the water content in liquid product decreases, and reason to this can be

attributed to the fact that with increase in severity the portion of tar also increases (Chen et al., 2018b). The HHV of liquid product obtained during torrefaction has been 9.79 and 10.21 MJ/kg for TPSO and TECO, respectively, which has been on the lower side due to the fact that they have been rich in oxygen and water content. Similar results were obtained by Chen et al. (Chen et al., 2018b) where HHV of liquid phase obtained after torrefaction of rice husk at 300^{o} C was around 8.7 MJ/kg.

To determine the main organic components present in the liquid product of the torrefaction process at optimum condition (TPSO and TECO), GC-MS analysis has been performed. It can be asserted that in the liquid product which has been obtained during the torrefaction process of biomass, the main dominating species present have been aldehydes, phenols, alcohol, and ketone. On analyzing Fig. 4.20 it can be observed that the maximum amount of organic compounds present has been the phenol derivatives (~ 34 and ~37 % for TPSO and TECO, respectively), and simple structural phenol have been obtained mainly due to hemicellulose decomposition (Yue et al., 2017). The other main component present has been furans derivatives like 2-furancarboxaldehyde (22.31%), which has been obtained from the dehydration along with the acid-catalyzed ring contraction reaction of pentosyl residue in hemicellulose and D-glucosyl residue present in cellulose (Wang et al., 2017a; Wang et al., 2017b). Ketones have been obtained in a liquid derivative of torrefaction process and these cyclic ketones as reported by other researchers were obtained from the secondary decomposition of cellulose (Wang et al., 2012). While linear ketones have been obtained from holocellulose decomposition which happens through ring scission, dehydration, decarboxylation, and rearrangements (Shen and Gu, 2009). Derivatives of acetic acid and esters (dibutyl phthalate) have been also obtained in appreciable

amounts where dibutyl phthalate can be utilized for plasticizer due to its low toxicity. The liquid product obtained from torrefaction can act a possible source of chemicals which are rich in oxygen containing functional groups. As many of the oxygen-containing chemicals are now being produced from fossil fuels using hydration or oxygenation of the olefins to introduce oxygen-containing functional groups (G. Clerici, 1991). On the other hand, these functional groups are present in huge amount in the liquid part obtained during the torrefaction of biomass (Czernik and Bridgwater, 2004).

Table. 4.8 HHV and water content of the liquid product obtained during torrefaction

Samples	HHV (MJ/kg)	Water content (wt.%)
TPS-200-0-5	6.91	84.3
TEC-200-0-5	7.43	81.4
TPSO	9.79	66.3
TECO	10.21	63.6
TPS-300-60-20	11.08	55.4
TEC-300-60-20	11.94	50.2

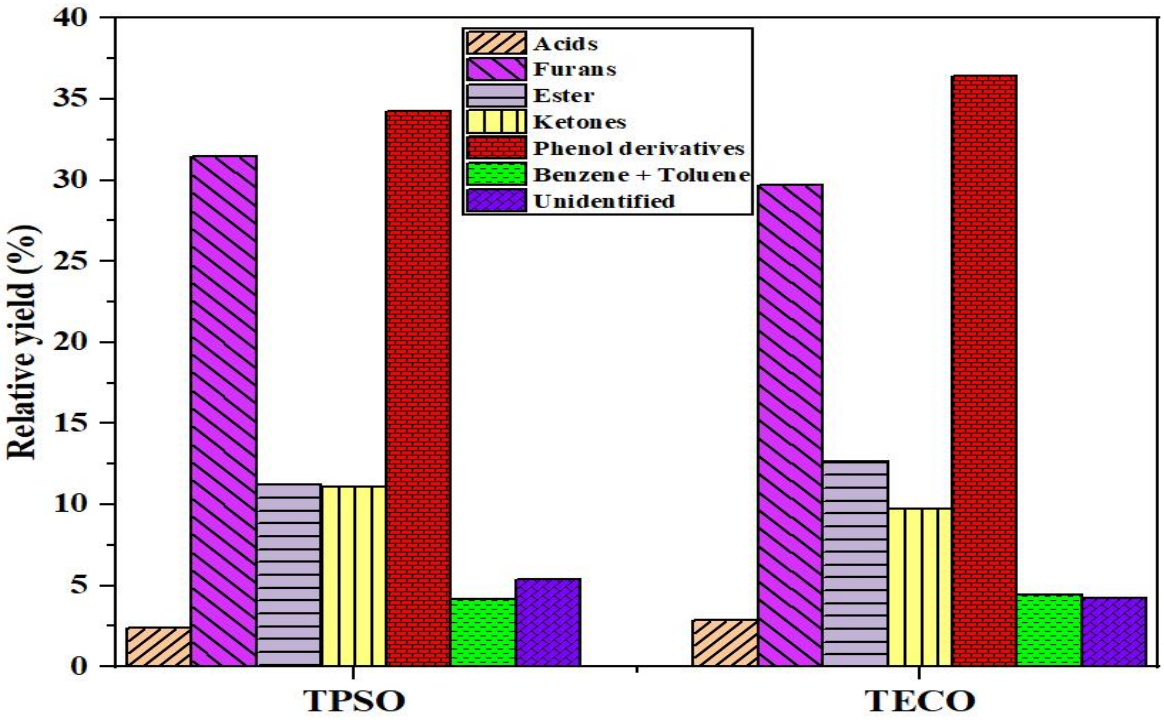

Fig. 4.20 Relative yield (%) of compound groups present in the liquid product.

4.14 Characteristics of the torgas (NCG) obtained during the torrefaction of biomass

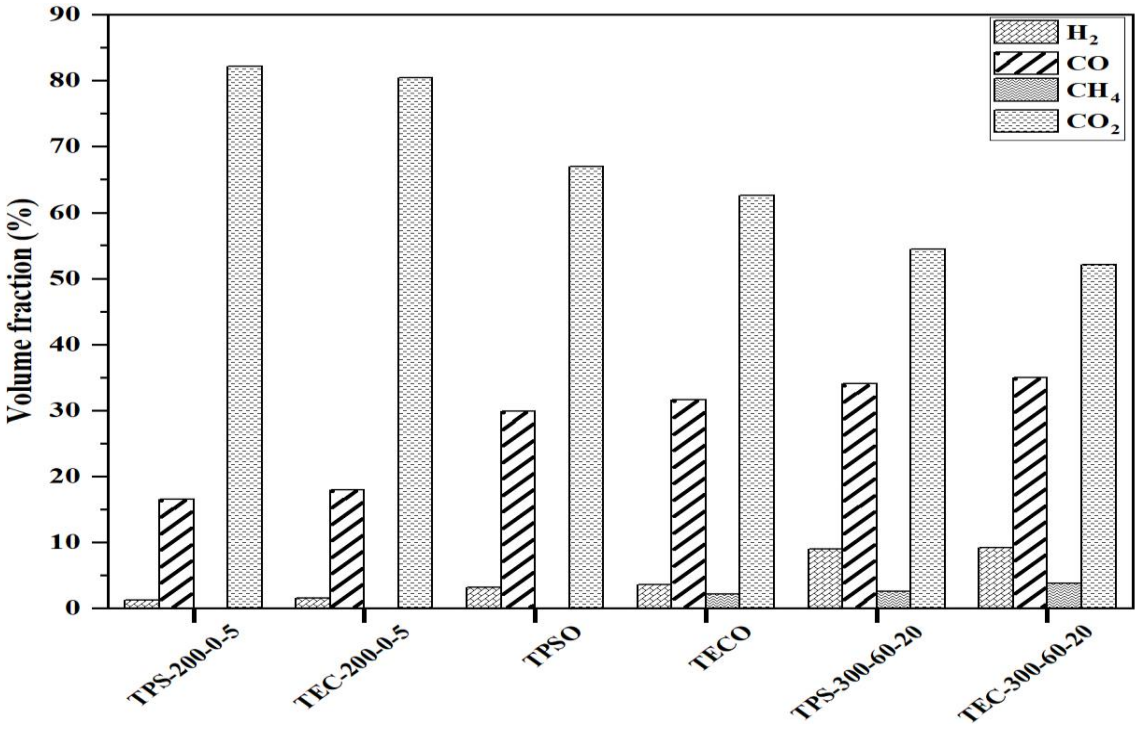

Fig. 4.21 Composition variation of torgas (N_2 free basis) with severity of torrefaction.

Samples of torgas (NCG) have been analyzed for the optimum conditions (TPSO and TECO) and compared with the least (TPS-200-0-5 and TEC-200-0-5) and most (TPS-300-60-20 and TEC-300-60-20) severe torrefaction conditions. Fig. 4.21 represents the gas composition (nitrogen free basis) in volume percentage for H_2, CO, CH_4, and CO_2. In Fig. 4.21 for TPS-200-0-5 and TPSO, CH_4 has been not detected because in few biomass the fragmentation of methoxy group present in lignin does not happen at low temperature and very minor demethylation of hemicellulose happens at mild and moderate torrefaction condition (Mohammed et al., 2017). At the optimum torrefaction condition (TPSO and TECO), the concentration of torgas have been CO_2 (66.95 and 62.58 %), CO (29.88 and 31.66 %), CH_4 (0 and 2.18%) and H_2 (3.17 and 3.58 %).

The high concentration of CO_2 and CO at all torrefaction conditions can be attributed to fragmentation and following the transformation of unstable carboxyl and carbonyl groups from depolymerization of hemicellulose and cellulose (Collard and Blin, 2014). It has been observed in Fig. 4.21 that the concentration of CO_2 decreases, and that of CO increases with increase in severity of torrefaction. This has been due to the reason as stated by Zhang et al. (Zhang et al., 2018) that during torrefaction as the severity increases decarbonylation reaction becomes stronger as compared to decarboxylation reaction. This can be further attributed to the fact that decarboxylation reactions are exothermic in nature, which can be supported even at low severity torrefaction. In contrast, decarbonylation reactions are mild endothermic, which at higher severity of torrefaction becomes more favorable which results in the increase of concentration for CO as compared to CO_2.

4.15 Summary

Based on the discussions held in this chapter it can be summarised that the solid fuel properties like HHV, FR, CI, and VI improved for the torrefied pigeon pea stalk and eucalyptus, thus making it compatible with the existing coal based power plants available in South Asian and African countries. FTIR analysis confirmed the removal of –OH groups during torrefaction process, making torrefied biomass more suitable for long term storage (raw biomass are highly hygroscopic) as compared to raw biomass. The kinetic parameters estimation revealed that the torrefaction reduced the overall activation energy for both moderate and severely torrefied biomass. GC-MS results suggested that further investigation can be done for the liquid product to extract some useful chemicals. The analysis of torgas revealed that it mostly consisted of CO_2 which was a lean energy gas and this also confirmed the removal oxygen from the biomass.